INTERNAL FRICTION IN COPPER-ALUMINUM ALLOYS DUE TO STRESS-INDUCED ORDERING

By

Donald E. Plumlee

A Thesis Submitted to the Faculty of the

DEPARTMENT OF MINING AND METALLURGICAL ENGINEERING

In Partial Fulfillment of the Requirements
For the Degree of

MASTER OF SCIENCE

In the Graduate College

UNIVERSITY OF ARIZONA

1963

STATEMENT OF AUTHOR

This thesis has been submitted in partial fulfillment of requirements for an advanced degree at the University of Arizona and is deposited in the University Library to be made available to borrowers under rules of the Library.

Brief quotations from this thesis are allowable without special permission, provided that accurate acknowledgment of source is made. Requests for permission for extended quotation from or reproduction of this manuscript in whole or in part may be granted by the head of the major department or the Dean of the Graduate College when in their judgment the proposed use of the material is in the interests of scholarship. In all other instances, however, permission must be obtained from the author.

SIGNED: Donald E. Plumlee

APPROVED BY THESIS DIRECTOR

This thesis has been approved on the date shown below:

D. J. Murphy
Professor of Metallurgy

10 May 1963
Date

ABSTRACT

A torsional pendulum apparatus was constructed for the investigation of internal friction in wire specimens. Torsional damping measurements were conducted on copper-rich alloys containing nominally 5 w/o and 9 w/o aluminum, respectively. Peak values of internal friction due to stress-induced ordering were found in these alloys at 431°C and 392°C at an oscillating frequency of .41 cycles per second.

ACKNOWLEDGEMENT

The author wishes to express his appreciation and thanks to the following persons: to Dr. D. J. Murphy for his helpful comments and suggestions on the presentation of this text, and to Mr. W. W. Walker for his assistance in the photographing of the equipment.

TABLE OF CONTENTS

Page

1. INTRODUCTION 1

2. REVIEW OF LITERATURE 2

2.1 Interstitial Stress-Induced Ordering 2
2.2 Substitutional Stress-Induced Ordering 4
2.3 Application of Stress-Induced Ordering to Diffusion . . . 6

3. OBJECTIVE 10

4. THEORETICAL CONSIDERATIONS 11

4.1 Relation Between the Internal Friction and the Ratio of the Amplitudes of Vibration in Free Decay for a Torsional Pendulum 11
4.2 Relation for the Determination of the Relaxation Time . . 17
4.3 Equation for the Elastic After-Effect 19

5. EXPERIMENTAL PROCEDURE 21

5.1 In General 21
5.2 Material 24
5.3 Apparatus 24

5.31 Torsional Pendulum One 24

5.311 Upper and Lower Supports 24
5.312 Heating Chamber 25
5.313 Pendulum 26
5.314 Furnace and Controls 27
5.315 Electromagnet and Controls 28
5.316 Light and Scale System 28

5.32 Torsional Pendulum Two 29

5.321 Furnace Support 29
5.322 Furnace and Controls 30
5.323 Furnace Caps 31
5.324 Pendulum 32
5.325 Electromagnet and Controls 33
5.326 Light and Scale System 34

Page

5.33 Modification of Torsional Pendulum Two for Elastic After-Effect Measurements. 35

5.4 Procedure. 35

5.41 Section One, Pertaining to Torsional Pendulum One. 36

5.411 Standardization of Thermocouple 36
5.412 Thermal Gradient in the Heating Chamber of Torsional Pendulum One. 36
5.413 Typical Experimental Run Using Torsional Pendulum One. 37

5.42 Section Two, Pertaining to Torsional Pendulum Two. 40

5.421 Thermal Gradient in Torsional Pendulum Two. 40
5.422 Typical Experimental Run Using Torsional Pendulum Two. 40
5.423 Elastic After-Effect Measurement. 42

6. RESULTS AND DISCUSSION. 45

6.1 In General 45
6.2 Section One, Pertaining to Torsional Pendulum One. . . . 45

6.21 Identification of Stress-Induced Ordering Peaks (T_1, θ_1, R_1) 45
6.22 Reproducibility of Curves. 47

6.3 Section Two, Pertaining to Torsional Pendulum Two. . . . 47

6.31 Elastic After-Effect Measurement (T_2, R_2). 47
6.32 Elastic After-Effect in Cu-15 a/o Zn 48
6.33 Annealing Treatments for Enlargement of Grain Size 49

6.4 Summary. 51

7. CONCLUSIONS 52

BIBLIOGRAPHY. 53

APPENDIX A A SAMPLE INTERNAL FRICTION CALCULATION 56

LIST OF TABLES

		Page
TABLE 1	SOME VALUES OF D_o AND ΔH DETERMINED BY ANELASTIC METHODS FOR DIFFUSION OF CARBON, NITROGEN, AND OXYGEN IN DILUTE B.C.C. INTERSTITIAL ALLOYS.	57
TABLE 2	COMPOSITION OF ALUMINUM BRONZES.	58
TABLE 3	SAMPLE EXPERIMENTAL DATA FOR A TORSIONAL MEASUREMENT .	59
TABLE 4	SAMPLE EXPERIMENTAL DATA FOR AN ELASTIC AFTER-EFFECT MEASUREMENT.	61

LIST OF FIGURES

Figure		Page
1	VECTOR DIAGRAM OF THE PHASE RELATIONSHIP BETWEEN STRESS AND STRAIN.	62
2	PLOT OF THE FACTOR $\frac{wR}{1 + w^2R^2}$ AGAINST ln wR.	62
3	SCHEMATIC DIAGRAM OF TORSIONAL PENDULUM ONE.	63
4	FRONT VIEW OF TORSIONAL PENDULUM ONE	64
5	FRONT VIEW OF INERTIAL CROSSMEMBER, MIRROR, AND ELECTROMAGNET OF TORSIONAL PENDULUM ONE.	65
6	SCHEMATIC DRAWING OF LIGHT AND SCALE SYSTEM.	66
7	SIDE VIEW OF SCALE	67
8	SCHEMATIC DIAGRAM OF TORSIONAL PENDULUM TWO.	68
9	FRONT VIEW OF TORSIONAL PENDULUM TWO	69
10	FRONT VIEW OF INERTIAL CROSSMEMBER, MIRROR, AND ELECTROMAGNETS OF TORSIONAL PENDULUM TWO	70
11	SCHEMATIC DIAGRAM OF METHOD USED TO TWIST SPECIMEN FOR AN ELASTIC AFTER-EFFECT MEASUREMENT.	71
12	FRONT VIEW OF FURNACE MODIFIED FOR ELASTIC AFTER-EFFECT MEASUREMENTS.	72
13	THERMAL GRADIENT IN HEATING CHAMBER OF TORSIONAL PENDULUM ONE	73
14	INTERNAL FRICTION CURVE OF A SPECIMEN (Cu-8.91 w/o Al) ANNEALED 30 HOURS AT 700°C (TORSIONAL PENDULUM ONE).	74
15	THERMAL GRADIENT IN HEATING CHAMBER OF TORSIONAL PENDULUM TWO	75
16	INTERNAL FRICTION CURVE OF A SPECIMEN (Cu-8.91 w/o Al) ANNEALED 50 HOURS AT 700°C (TORSIONAL PENDULUM TWO) .	76
17	ELASTIC AFTER-EFFECT CURVE OF A SPECIMEN (Cu-8.91 w/o Al) (ANNEALED 50 HOURS AT 700°C) MEASURED AT 340°C	77

Figure		Page
18	INTERNAL FRICTION CURVE OF A SPECIMEN (Cu-8.91 w/o Al) ANNEALED 2 HOURS AT 500°C (TORSIONAL PENDULUM ONE). . . .	78
19	INTERNAL FRICTION CURVE OF A SPECIMEN (Cu-8.91 w/o Al) ANNEALED 50 HOURS AT 700°C (TORSIONAL PENDULUM ONE) . . .	79
20	INTERNAL FRICTION CURVE OF A SPECIMEN (Cu-4.91 w/o Al) ANNEALED 50 HOURS AT 700°C (TORSIONAL PENDULUM ONE) . . .	80
21	RE-MEASUREMENT OF INTERNAL FRICTION CURVE OF SPECIMEN (Cu-8.91 w/o Al) ANNEALED 50 HOURS AT 700°C (TORSIONAL PENDULUM ONE)	81
22	GRAIN SIZE OF SPECIMEN (Cu-8.91 w/o Al) ANNEALED 50 HOURS AT 700°C USED IN SECTION ONE.	82
23	INTERNAL FRICTION CURVE OF A SPECIMEN (Cu-4.91 w/o Al) ANNEALED 24 HOURS AT 950°C (TORSIONAL PENDULUM TWO) . . .	83
24	SAMPLE PLOT OF A SET OF SCALE READINGS ON SEMI-LOG PAPER.	84
25	ELASTIC AFTER-EFFECT CURVE OF A Cu-15 a/o Zn SPECIMEN (ANNEALED 48 HOURS AT 750°C) MEASURED AT 260°C	85

1. INTRODUCTION

The capacity of a vibrating solid to convert its mechanical energy of vibration into heat is called internal friction. Interest in internal friction undoubtedly dates back to prehistoric times, to the earliest cymbals and bells. In modern times, the study of internal friction has followed two branches: one has been the study of damping for engineering applications, and the second has been the use of damping as a tool to study internal structure and atomic movements in solids (1).

In the latter field of study, anelasticity, which is concerned with internal friction effects that are independent of the amplitude of vibration, i.e., which result in non-permanent deformation of a specimen, has proved to be one of the most important. Many experimentally observable effects have been shown to manifest anelastic behavior. Among these are thermal diffusion, atomic diffusion, stress relaxation across grain boundaries, magnetic interactions, and stress-induced ordering (2). It is the latter, the effect of stress-induced ordering, which has been studied in the present investigation.

2. REVIEW OF LITERATURE

2.1 Interstitial Stress-Induced Ordering

In 1939, Snoek (3) reported that the previously known temperature-and-frequency-dependent damping peak of alpha-iron disappeared when all traces of carbon and nitrogen were removed, and that the peak reappeared upon reintroducing carbon and nitrogen. Later in 1941, Snoek (4) reported that the height of the peak was proportional to the interstitial concentration and suggested a mechanism to explain the peak's origin.

Snoek theorized that interstitial atoms of carbon and nitrogen in b.c.c. (body-centered cubic) iron were not located in the largest spaces available to them, but at the centers of the cell edges and at the face centers, which are equivalent positions. Under such conditions, an interstitial atom located in one of these positions would distort the lattice, and the distortion would be most pronounced in the direction of the two closest iron atoms.

Under zero stress, the interstitial sites would be occupied in a random fashion, but upon application of a stress in one of the $\langle 100 \rangle$ directions, the atoms in sites aligned with the major stress axis would experience a lowering of their energy compared to the atoms in the other sites. Under the above conditions, the interstitial atoms would preferentially distribute themselves along the major stress axis. The energy required for the atoms to preferentially realign themselves in

the solid would then be observed as an increase in internal friction in the solid.

Dijkstra (5) verified Snoek's theory using single crystals of alpha-iron. By Snoek's theory, if a stress is applied along one of the <111> directions, then all the interstitial axes are equally inclined to the stress axis. Thus, no preferential sites for interstitial atoms are formed to cause stress-induced ordering. Dijkstra found that the internal friction in alpha-iron for a stress applied in one of the <111> directions was only five per cent of that for a stress applied in one of the <100> directions.

After Snoek's experiments, other b.c.c. metals were investigated and found to have the same type of damping peak due to stress-induced ordering of interstitial carbon, nitrogen, or oxygen. Table 1 lists some of the interstitial alloys that have been investigated.

Dilute f.c.c. (face-centered cubic) interstitial alloys do not manifest the above anelastic effect. However, anelastic effects have been observed in martensitic low carbon nickel steels (6), and relatively concentrated alloys such as 1.34 atomic per cent (a/o)C in f.c.c. iron stabilized with Mn (7). In the latter, the anelastic effect is thought to arise from the difference in length of the Mn-C and the Fe-C bond. If the M-C bond is different (either longer or shorter) than the Fe-C bond, then under an applied stress certain interstitial sites become favored, and therefore, ordering takes place.

2.2 Substitutional Stress-Induced Ordering

In 1943, Zener (8) reported an anomalous damping peak in the substitutional solid solution alpha-brass (30 a/o Zn) with properties much like those of the stress-induced ordering peak in interstitial solid solutions.

In 1947, Zener (9) suggested a mechanism to explain the peak's origin. In a cubic lattice, a single solute atom which is larger or smaller than the solvent atoms around it will distort the cubic symmetry. The distortion, however, may be expected to be homogeneous in the various crystallographic directions. There are, therefore, no preferential sites for such atoms when a stress is applied, as in the interstitial case. The distortion, however, about a pair of solute atoms in nearest neighbor positions is no longer homogeneous in the cubic sense. A pair of solute atoms will produce asymmetric distortion about the direction of the pair axis. Thus, pairs of substitutional solute atoms would behave in a manner analogous to single interstitial atoms.

When a stress is applied in some crystallographic direction, the pair axes will show a preferential alignment in those crystallographic directions which are nearest to the stress direction. The energy required for the pair axes to preferentially realign themselves in the solid would then be observed as an increase in internal friction in the solid.

From the above model, the magnitude of the internal friction should be proportional to the number of solute pairs, which in turn

should be proportional to the square of the solute concentration (10). Berry (11) confirmed this square law dependence for aluminum-copper solid solutions below 1.8 a/o Cu which suggests the validity of the pair concept at low concentrations.

At higher concentrations, larger aggregates than isolated pairs of solute atoms would be expected so that Zener's "pair reorientation model" would no longer be applicable. Le Clare and Lomer (12) suggested the "directional ordering model." Le Clare and Lomer theorized that a short-range order parameter might be assigned to each of the z/2 nearest-neighbor directions of the crystal (z being the coordination number). Under zero stress all of these parameters would be equal, but under an applied stress, the equilibrium value of these parameters would no longer be equal to one another and a readjustment of atomic configuration would take place. The energy required for the readjustment of the atomic configuration in the solid would then be observed as an increase in internal friction in the solid.

Both Zener's "pair reorientation model" and Le Clare and Lomer's "directional ordering model" predict that the internal friction is zero for a stress applied in the $[100]$ direction and a maximum for a stress applied in the $[111]$ direction for a b.c.c. lattice. However, work by Seraphim and Nowick (13) on b.c.c. Li-Mg solid solutions and Artman (14) on beta-brass has shown the reverse to be true.

Therefore, at the present time there is no satisfactory explanation of the Zener Effect, which reflects not an inherent defect in the theory of anelasticity, but, simply inadequate knowledge of solid

solutions themselves. However, Seraphim and Nowick (13) have pointed out that the above observed effects may be explained with the assumption that only next-nearest-neighbors instead of nearest-neighbors need be considered. With the above assumption, the internal friction would be greatest in the [111] direction and zero for the [100] direction for a b.c.c. lattice.

2.3 Application of Stress-Induced Ordering to Diffusion Measurements

In experimental diffusion work, the use of radioactive tracers has been highly successful in extending conventional methods and in providing new techniques for determining diffusion coefficients. This approach, however, has not solved all problems. Many processes occur in metals and alloys by the mechanism of diffusion at low temperatures for which the diffusion coefficient must be extrapolated from high temperature results, an extrapolation which often is not warranted (15). The phenomenon of stress-induced ordering then provides a new means for determining the temperature dependence of the diffusion coefficient in binary solid solutions below the temperature range in which regular diffusion experiments are feasible. Low temperature internal friction diffusion data combined with regular high temperature data then provides the best possible value for the diffusion coefficient over the complete temperature range (16).

An extensive study from existing data and original work was made of diffusion in interstitial alloys of carbon and nitrogen in alpha-iron, and carbon, nitrogen, and oxygen in tantalum by Wert (17) (18) and Wert and Zener (19). With the atomic model for the relaxation

process in interstitial alloys known, an exact relationship between the diffusion coefficient D and the relaxation time R was determined. It was found that the mean time between successive jumps of a given atom J was related to the relaxation time R by the expression

$$J = \frac{3}{2} R \tag{1}$$

while the diffusion coefficient D was related to the mean time between successive jumps of a given atom by the expression

$$D = \frac{a^2}{12J} \tag{2}$$

where a is the lattice parameter and 1/12 a geometric constant calculated from the atomic configuration. Therefore, the relationship

$$D = \frac{a^2}{36R} \tag{3}$$

which has been found applicable for all dilute b.c.c. interstitial alloys, may be written. Table 1 lists the constant D_o and the activation energy ΔH for various interstitial alloys determined by anelastic methods.

Since the exact atomic model for relaxation in substitutional alloys is not yet known, a relationship comparable to that for interstitial alloys cannot be written. Therefore, various investigators have attempted to determine an empirical relationship corresponding to Equation 3, that is

$$D = B \frac{a^2}{R} \tag{4}$$

where B is a constant in which it is hoped the number connecting R to J and the number connecting J to D is contained. To find B, D is first measured by conventional methods (chemical gradient or radioactive tracer) and then R is measured for the same alloy by anelastic methods. With both types of data obtained, the constant B is then determined by fitting the two types of data to each other. The above method requires that D and 1/R have the same temperature dependence, i.e., the same activation energies. This has been found approximately true so that attempts to find a relationship between D and R do have significance (20).

Hino, Tomizuka, and Wert (15) have carried out the most complete investigation of this type on alpha-brass. First, radioactive tracers of copper and zinc were diffused into 31 percent alpha-brass single crystals. The activation energies for D_{Zn} and D_{Cu} were found to be 40,700 cal per mole and 41,900 cal per mole. From the anelastic measurements, the activation energy relating the relaxation times was found to be 37,800 cal per mole. Both the diffusion and anelastic measurements are thought accurate enough so that the difference in activation energies of about 3,000 cal per mole between R and D_{Zn} and 4,000 cal per mole between R and D_{Cu} are significant. Fitting the data between R and D_{Zn} at about 580°C, the value of B is found to be 1/14, which, for a f.c.c. lattice is about the same value for the constant as 1/36 is for the b.c.c. interstitial lattice.

The same type of measurements have been carried out for an alloy of Ag containing 30 a/o Zn by comparing the diffusion data of Lazarus and Tomizuka (21) with the anelastic data of Nowick (22). Here again a

discrepancy of about 3,000 cal per mole was found between the activation energies from the tracer diffusion and the anelastic effects. Fitting the data between R and D_{Zn} at about 600°C, the value of B was found to be 1/16.

However, Turner and Williams (23) have obtained very good agreement between the data for tracer diffusion of Ag into a 68 a/o Au-Ag alloy and their own anelastic data for the same alloy by setting

$$B = \frac{f}{12} \tag{5}$$

where f is the Bardeen and Herring (24) correlation factor.

For b.c.c. lattices, the tracer diffusion data of Kuper, Lazarus, Manning, and Tomizuka (25) has been compared to the anelastic data of Artman (14) on partially ordered beta-brass. No extrapolation of either data was required to fit the data together at about 315°C. A value for B of about 1/25 was found.

3. OBJECTIVE OF INVESTIGATION

In extensive investigations of the internal friction characteristics of Cu-rich alloys of the Cu-Zn system, a temperature dependent stress-induced ordering effect has been reported.

The similarity of the Cu-rich end of the Cu-Al phase diagram to that of the Cu-Zn diagram and the fact that such Cu-rich alloys in both systems are substitutional solid solutions have suggested that a similar stress-induced ordering effect might be observed in Cu-Al.

The objective of this thesis, therefore, was to determine whether such a stress-induced ordering effect exists in representative aluminum alloys of copper, and, if so, the temperature dependence thereof.

4. THEORETICAL CONSIDERATIONS

Equations for the anelastic effect of stress-induced ordering are developed in the following sections. The development of the equations applies to the specific type of equipment and materials used in the present investigation.

4.1 Relation Between the Internal Friction and the Ratio of the Amplitudes of Vibration in Free Decay for a Torsional Pendulum

In the present investigation, the specimen forms part of the suspension element of a torsional pendulum, and in accord with previous work of other investigators, the strain is assumed to be uniform over the length of the specimen. This condition may be realized for a torsional pendulum by the use of an auxiliary inertial member, to which by comparison, the inertia of the specimen is negligible (1).

The total strain, e, in the specimen is assumed to be made up of two parts (1):

$$e = e' + e'' \tag{1}$$

e' is the perfectly elastic component of strain which obeys Hooke's law

$$e' = \frac{s}{M} \tag{2}$$

where s is the applied stress and M is the modulus of elasticity, and e'' is the non-elastic strain which results from the internal reordering.

In order for internal friction to occur in the specimen, the stress and strain must be out of phase with each other, and, for energy to be dissipated, the strain must lag behind the stress as in any hysteresis condition (1).

Figure 1 is a vector diagram of the phase relationship between the applied stress, s, and resultant strain, e:

1. s is the vector representation of the total stress.
2. e is the vector representation of the total strain out of phase with stress by lag angle θ.
3. e' is the vector representation of the perfectly elastic component of strain in phase with stress.
4. e'' is the vector representation of the non-elastic component of strain out of phase with stress.
5. e_1'' is the vector representation of the component of non-elastic strain in phase with stress.
6. e_2'' is the vector representation of the component of non-elastic strain out of phase with stress.

The lag angle θ by which the strain lags the stress is a convenient measure of internal friction, since the energy dissipated in a cycle of vibration goes to zero when θ approaches zero. The damping is assumed to be small (1) so that

$$\tan \theta \tilde{=} \theta \qquad (3)$$

The following relation may then be written for the internal friction (Figure 1):

$$\theta = \frac{e_2''}{e' + e_1''} \tag{4}$$

Using complex notation, the oscillatory stress may be written as (Figure 1)

$$s.\exp(iwt) \tag{5}$$

where w is the angular frequency of vibration, t is the time, and i is the $\sqrt{-1}$. Further, the oscillatory elastic strain may be written as

$$e'.\exp(iwt) \tag{6}$$

and the oscillatory non-elastic strain as

$$e''.\exp(iwt) = (e_1'' - ie_2'').\exp(iwt) \tag{7}$$

The complex elastic modulus M_c is defined as the oscillatory stress divided by the oscillatory elastic and non-elastic strains, therefore,

$$M_c = \frac{s.\exp(iwt)}{e'.\exp(iwt) + (e_1'' - ie_2'')\exp(iwt)} \tag{8}$$

or

$$M_c = \frac{s}{(e' + e_1'')\left[1 - \frac{ie_2''}{e' + e_1''}\right]} \tag{9}$$

The dynamic elastic modulus M_d is defined as the oscillatory stress divided by the oscillatory elastic and non-elastic strains in

phase with stress. Using complex notation, the total oscillatory strain in phase with stress may be written (Figure 1)

$$(e' + e'') \cdot \exp(iwt) \tag{10}$$

The dynamic modulus M_d may be written as

$$M_d = \frac{s \cdot \exp(iwt)}{(e' + e_1'') \cdot \exp(iwt)} \tag{11}$$

or

$$M_d = \frac{s}{(e' + e_1'')} \tag{12}$$

Substituting Equations 4 and 12 into Equation 9, the relation for the complex elastic modulus M_c becomes

$$M_c = \frac{M_d}{1 - i\theta} \approx M_d(1 + i\theta) \tag{13}$$

Then upon substituting Equations 1, 7, and the above relation for the complex elastic modulus M_c into Equation 8, the relation between the total stress, s, and the total strain, e, may be found, which is

$$s = M_d(1 + i\theta)e \quad (1) \tag{14}$$

The torque τ of the auxiliary inertial member is equal to the product of the moment of inertia I and the acceleration α.

$$\tau = I\alpha = I \frac{d^2\phi}{dt^2} \tag{15}$$

where ϕ represents the angle of twist in the specimen. For a freely decaying pendulum, the torque τ must equal the restoring torque M_t,

which is exerted upon the auxiliary inertial member by the specimen, but opposite in sign. The equation of motion of the torsional pendulum then becomes

$$I \frac{d^2\phi}{dt^2} = -M_t \tag{16}$$

The quantity ϕ is essentially the shearing strain e throughout the specimen except for a constant of proportionality. The shearing strain, e, of the specimen is equal to the product of the radius, r, of the specimen and the angle of twist, ϕ, divided by the length of the specimen, L (26).

$$e = \frac{r}{L} \phi \tag{17}$$

Similarly, the restoring torque, M_t, is equal to the product of the shearing stress, s, and the polar moment of inertia, I_p, divided by the radius, r, of the specimen (26).

$$M_t = \frac{I_p}{r} s \tag{18}$$

Substituting Equations 14, 17, and 18 into Equation 16 gives

$$\frac{d^2e}{dt^2} + \frac{I_p M_d}{IL} (1 + i\theta)e = 0 \tag{19}$$

A measure of the magnitude of the damping is the loss of amplitude per cycle. Thus, a convenient method of measuring the internal friction, θ, is in terms of d, the ratio of the amplitudes of vibration. The damping per cycle of vibration is

$$\frac{d}{2\pi} \tag{20}$$

Therefore, it is convenient to assume a particular solution of the following form for Equation 19 (1):

$$e = e_o.\exp(-\frac{d}{2\pi}wt).\exp(iwt) \tag{21}$$

which represents exponentially damped vibrations (e_o is the initial strain). Substituting Equation 21 into Equation 19 gives

$$(i^2 - i\frac{d}{\pi} + \frac{d^2}{4\pi^2})w^2 + \frac{I_p M_d}{IL}(1 + i\theta) = 0 \tag{22}$$

Setting

$$\frac{I_p M_d}{IL} = w^2 \tag{23}$$

and then solving for θ gives

$$\theta = \frac{d}{\pi} - \frac{d^2}{4\pi^2 i} \tag{24}$$

Equation 19 thus has the solution

$$e = e_o.\exp(-\frac{d}{2\pi}wt).\exp(iwt) \tag{21}$$

when Equations 23 and 24 are satisfied. Neglecting the second order term in Equation 24, the required relation found is

$$d = \pi\theta \tag{25}$$

The ratio of the amplitudes of vibration d is equal to the product of π and the internal friction θ (1).

4.2 Relation for the Determination of the Relaxation Time

Following the approach of Nowick (1) and starting with a state of random atomic order in the specimen under conditions of zero stress, the fractional degree of ordering of atoms produced by application of the applied stress s at a particular time will be designated by N. The following three conditions are then assumed to apply:

1. The non-elastic strain, e", is proportional to N.

$$e'' = kN \tag{26}$$

where k denotes the proportionality constant.

2. The equilibrium value of N, denoted by $\bar{N}$, is proportional to the applied stress s

$$s = c\bar{N} \tag{27}$$

where c denotes the proportionality constant.

3. The degree of equilibrium order attained through the application of constant stress is $\bar{N} - N$ and requires time R (relaxation time) to be achieved. The rate of change of order is then expressed by the following relaxation equation.

$$\frac{dN}{dt} = -\frac{(N - \bar{N})}{R} \tag{28}$$

From condition 1, the equilibrium non-elastic strain, $\bar{e}''$, is proportional to the equilibrium value of N.

$$\bar{e}'' = k\bar{N} \tag{29}$$

The applied stress, s, is also proportional to the equilibrium value of N (Equation 27), and therefore, $\bar{e}''$ is also proportional to the applied stress, s. Substituting Equation 2 for the applied stress, s, the above equilibrium non-elastic strain, $\bar{e}''$, may be written proportional to the elastic strain, e'.

$$\bar{e}'' = ue' \tag{30}$$

where u denotes the proportionality constant. Substituting Equations 26, 29, and 30 into Equation 28, the relaxation equation may now be written in terms of the elastic and non-elastic strains e' and e''.

$$\frac{de''}{dt} = -\frac{(e'' - ue')}{R} \tag{31}$$

Using the above relation, the frequency dependence of the internal friction due to stress-induced ordering may be found by substituting the oscillatory elastic strain (Equation 6) and non-elastic strain (Equation 7) into it.

$$\frac{(e_1'' - ie_2'')}{e'} = \frac{u}{(1 + iwR)} \tag{32}$$

Separating the real and imaginary parts and equating them separately,

$$\frac{e_1''}{e'} = \frac{u}{(1 + w^2R^2)} \tag{33}$$

and

$$\frac{e_2''}{e'} = \frac{uwR}{(1 + w^2R^2)} \tag{34}$$

Using the assumption that the non-elastic strain is small, Equation 4 may be written as

$$\theta = \frac{e_2''}{e'} \tag{35}$$

The relation between the internal friction, θ, the angular frequency of vibration, w, and the relaxation time, R, may then be found by substituting the above relation for θ into Equation 34.

$$\theta = \frac{uwR}{(1 + w^2R^2)} \tag{36}$$

Graphing the factor $\frac{uwR}{(1 + w^2R^2)}$ against ln wR gives a symmetrical function with the general characteristics of an error curve (Figure 2). From the curve, it can be seen that

$$\theta_{max} = \frac{1}{2} u \tag{37}$$

when

$$\underline{wR = 1} \tag{38}$$

From Equation 38, the relaxation time R may be determined for the peak value of the internal friction peak when the angular frequency of vibration w is known (2).

4.3 Equation for the Elastic After-Effect

Upon substituting Equations 1 and 2 into Equation 31, the relation between the total stress, s, and the total strain, e, under conditions of constant stress may be found.

$$(1 - u)s + R\frac{ds}{dt} = M(e + R\frac{de}{dt}) \tag{39}$$

A solid which obeys Equation 39 is called a "standard linear solid" because it is linear in its stress and strain and in their first time derivatives (2).

When the twisting couple is removed in an elastic after-effect measurement, the applied stress, s, is then zero so that Equation 39 becomes

$$e + R\frac{de}{dt} = 0 \tag{40}$$

A solution is obtained by separating the variables

$$\frac{de}{e} = -\frac{dt}{t} \tag{41}$$

integrating both sides

$$\ln e + c_1 = -\frac{t}{r} + c_2 \tag{42}$$

and then adjusting the constants

$$e = c_3 \cdot \exp(-\frac{t}{R}) \tag{43}$$

The constant c_3 may be evaluated at $t = 0$ and $e = e_o$ so that Equation 43 may be written as

$$\underline{e = e_o \cdot \exp(-\frac{t}{R})} \tag{44}$$

where e is the strain, e_o is the initial strain, t is the time, and R is the relaxation time (22).

5. EXPERIMENTAL PROCEDURE

A description of the material, apparatus, and procedure used is given in the following sections. It should be noted that there was a three-year interval of military service which interrupted the continuity of the investigation reported upon in this thesis. As a result, upon resumption of the research after the interruption, completely new apparatus had to be built and much of the experimental work repeated. For purposes of clarity, the earlier and later apparatus and procedures are described under titles of Torsional Pendulum One and Torsional Pendulum Two.

5.1 In General

The act of twisting wire specimens in torsion introduces in them internal elastic stresses. Upon release of the twisting restraint, these stresses are permitted to relax. Such relaxation has been attributed to several processes, including stress relaxation across grain boundaries, stress relaxation due to stress-induced ordering, and others. The operation of these relaxation processes varies with imposed conditions. Some predominate under one set of conditions and some under others. Careful selection of experimental conditions, such as frequency of oscillation, temperature, and specimen structure may reveal the nature of a particular process of interest.

As previously indicated, the relaxation process of particular interest in this investigation was that due to stress-induced ordering. The experimental approach employed sought, by appropriate selection of conditions, to minimize the influence of other effects, to identify the particular effect, and to determine the temperature dependence of its relaxation time.

For a given composition, the relaxation time was sought by two types of measurement, torsional damping and elastic after-effect. The observation of torsional damping at a series of temperatures is capable of revealing a particular temperature T_1, at which the damping or internal friction achieves a maximum value as shown schematically in Sketch A below. An associated value of the relaxation time R_1 can be readily determined.

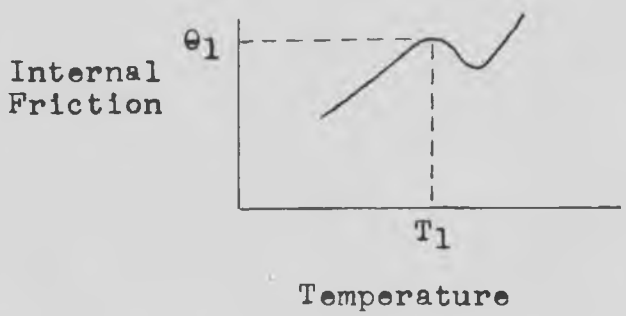

SKETCH A

The observation of the recovery from an applied elastic twisting strain, the elastic after-effect, is capable of revealing for a particular temperature T_2, the corresponding value of relaxation time, R_2, the time required for the strain to decrease to 1/e of

its original value, as shown schematically in Sketch B below.

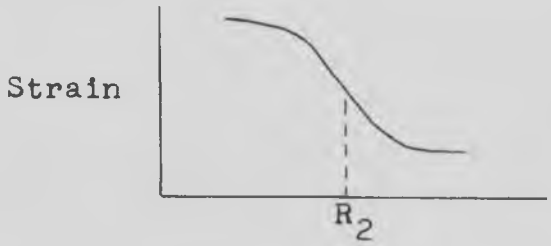

SKETCH B

A combination of values of this type can be plotted as in Sketch C below to show the dependence of the relaxation time on temperature.

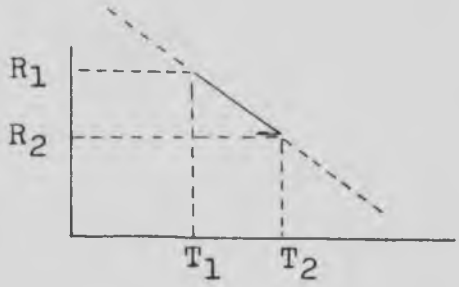

SKETCH C

The experimental procedure followed was directed toward obtaining the relationship indicated in Sketch C for each of two alloys of copper, one containing nominally 5 w/o aluminum and the other 9 w/o aluminum.

5.2 Material

The two alloys employed were commercial aluminum bronzes containing 4.91 and 8.91 per cent by weight (w/o) of aluminum in copper respectively, and were used in the form of wire approximately .035 inches in diameter. Metallographic examination showed the wire to be initially in the cold-worked condition as a result of previous drawing operations. The detailed composition of the two alloys is shown in Table 2.

5.3 Apparatus

5.31 Torsional Pendulum One

Both torsional pendulums used in the present investigation were patterned basically after one described by Ke (27). Figure 3 shows a schematic diagram of Torsional Pendulum One.

5.311 Upper and Lower Supports

To provide a solid support, the upper frame work, consisting of 2 by 4 inch boards, was bolted to the wall (Figure 4). This frame work supported the heating chamber and pendulum and was mounted at a sufficient height on the wall so that the specimen could be attached or removed from the pendulum through the bottom of the heating chamber.

The lower support was built to serve two purposes: the first was to support the furnace, and the second was to provide a frame work in which to enclose the inertial crossmember and thus prevent extraneous air currents in the room from introducing errors in the experimental

readings by swaying the pendulum. The removable front panel of the enclosure (not shown in figures) was provided with a rectangular opening so that the beam of light from the lighting system could be projected onto the mirror attached to the lower support element of the pendulum.

5.312 Heating Chamber

The heating chamber consisted of a stainless steel tube 2 feet in length and 2 inches in inside diameter with 3/16 inch wall thickness, which was attached to the upper frame work by two eccentric pieces of metal. This method of attachment was used because it provided a method of centering the lower support element of the pendulum in the hole in the lower cap.

The stainless steel tube was threaded so that metal caps could be screwed to each end. In the upper cap of the heating chamber, a square hole 1/2 inch by 1/2 inch was machined to fit the bearing block of the upper support element of the pendulum. An additional piece was machined and attached to the upper cap to provide additional bearing surface. This prevented the upper support element from turning in the upper cap.

This method of attachment, in conjunction with the counter weight system of the pendulum, provided an easy way of lowering the pendulum out through the bottom of the heating chamber for the purpose of attaching or removing the specimen.

An additional hole was drilled in the upper cap so that a chromel-alumel thermocouple could be inserted into the heating chamber

from the top.

In the lower cap of the heating chamber, a 1/4 inch diameter hole was drilled to provide passage for the lower support element of the pendulum. The 1/4 inch hole provided for 1/32 of an inch clearance on all sides between the lower support element of the pendulum and the side of the hole in the lower cap.

5.313 Pendulum

The pendulum consisted of two parts:

1. The upper support element and counter weight system.
2. The lower support element and inertial crossmember.

The upper support element was constructed in the following manner. A steel bearing block 2 1/4 inches long by 1/2 inch by 1/2 inch cross section was machined to fit the hole through the upper cap of the heating chamber. A stainless steel tube 3/16 of an inch in outside diameter with 1/32 of an inch wall thickness and 3 inches in length was connected to the lower side of the bearing block. To this tube in turn, a small pin vise 3 inches in length was attached. To the upper side of the bearing block, a stainless steel tube of the same cross sectional dimensions as the above but 7 1/2 inches long was then connected (Figure 3). This upper tube was drilled so that a cord could be attached to the top end to counter-weight the whole pendulum through a system of weights and pulleys (Figure 4).

Similarly, the lower support element and inertial crossmember was constructed in the following manner. A small pin vise 3 inches

long was connected to a stainless steel tube 8 1/2 inches long and of the same cross sectional dimensions as the above. An aluminum fitting held to the above stainless steel tube by an inset screw was then machined to hold the two inertial crosspieces. Each inertial crosspiece consisted of a piece of aluminum rod 1/8 inch in diameter and 10 1/2 inches long. To the outside ends of the inertial crosspieces, an aluminum collar threaded on the outside was slip-fitted. Two iron nuts were then screwed onto each collar (Figure 5).

These iron nuts provided the additional weight needed for the inertial crossmember as well as magnetic material for an electromagnetic starting device to act upon. Further, the nuts could be screwed back and forth on the collars so that the pendulum could be dynamically balanced.

A small mirror 1/2 inch long by 1/4 inch wide was glued to the stainless steel tube of the lower support element of the pendulum. The mirror was used in conjunction with the lighting system to measure the amplitude of vibration of the pendulum. The total weight of the lower support element and inertial crossmember of the pendulum, including the mirror, was 64 grams. During operation, the bottom end of the lower support element of the pendulum was dipped into a beaker of oil to damp out any lateral vibrations of the pendulum.

As can be seen from Figure 3, the specimen formed part of the suspension element of the pendulum. The specimen was connected between the pin vises of the upper and lower support elements of the pendulum.

5.314 Furnace and Controls

Around the stainless steel heating tube, an electrical

resistance furnace was mounted to provide heat for raising the temperature of the specimen. The furnace was controlled by a variable transformer, and, with this arrangement, a wide range of temperatures could be obtained.

5.315 Electromagnet and Controls

A small electromagnet powered by a 1 1/2 volt dry battery was mounted to the back wall of the enclosure directly behind the right end of the inertial crossmember. Oscillation of the pendulum was induced by momentarily activating the electromagnet through a tap key so that it attracted the two iron nuts on the right inertial cross piece.

5.316 Light and Scale System

The amplitude of vibration of the pendulum was measured with a scale and light system (Figure 6).

On a small wooden frame, a 6-volt bulb was mounted in a metal cup. The current for the bulb was provided by a small transformer which stepped the 110 volt wall current down to 6 volts. To act as the marker for reading the scale, a small wire .002 of an inch in diameter was mounted in the metal cup just in front of the filament of the bulb. A collimator and convex lens were then mounted on the wooden frame in front of the cup (Figure 4). By adjusting the light, the image of the wire could be projected onto the mirror attached to the lower support element of the pendulum so that it was reflected and focused on the scale 3 meters away from the pendulum.

A curved scale (curved to fit a 6 meter diameter circle) mounted on a stand was used with the above lighting system. The scale was divided in the metric system with the smallest division being one millimeter (Figure 7).

5.32 Torsional Pendulum Two

Torsional Pendulum Two, the improved version of Pendulum One, was also patterned basically after the one described by Ke (27). Figure 8 shows a schematic diagram of the torsional pendulum.

5.321 Furnace Support

The furnace support was built of sufficient height so that the specimen could be attached or removed from the pendulum through the bottom of the furnace (Figure 9).

The two ends of the furnace support consisted of 2 by 4 inch boards bolted together. The two ends were connected by four 15 inch lengths of angle iron. The two top pieces of angle iron were mounted with the angle up so that the bottom of the furnace would just fit between them and be held firmly in place. Two holes were drilled and threaded in each of the two top pieces of angle iron. By screwing the bolts placed in these holes up or down, the furnace could be leveled and the lower support centered in the hole through the lower cap. Foam rubber was then mounted to the bottom of the support to reduce extraneous vibrations.

5.322 Furnace and Controls

The furnace was constructed specifically for Torsional Pendulum Two. The furnace core consisted of an alumina tube 2 feet 1 inch in length with a 1 inch inside diameter. The heating element, consisting of standard high resistance wire, was wound on the alumina tube in three parts each 8 inches in length. The top section was wound with 7 1/2 turns per inch, the middle section with 7 turns per inch, and the bottom section with 8 turns per inch. The furnace was wound in this way for the purpose of reducing thermal gradients. The two end coils were then connected in series, separate from the center coil. A refractory cement was spread over the heating coils to hold them in place and to protect them from the outer insulation. This insulation consisted of ground fire brick which filled the remaining cavity within the 8 inch diameter galvanized tube which made up the outer wall of the furnace.

The furnace ends consisted of three 1/4 inch thick sheets of asbestos board 1 foot square bolted together. A 1 inch hole was drilled in the center of each of the furnace ends to accept the central alumina tube. Through four additional 1/4 inch diameter holes, four threaded tie rods were used to hold the furnace together.

The electrical leads for the heating coils were brought through small holes drilled in the furnace wall. The terminals were mounted on small 2 inch square blocks of asbestos board.

The two heating coils in the furnace (center and the two ends) were controlled by separate variable transformers. With this arrangement, temperatures up to 1000^{o}C could be obtained. A uniformity of

temperature of $\pm 4\frac{1}{2}^{o}C$ was recorded over the central 10 inch length at a working temperature of $392^{o}C$; a temperature corresponding to the middle of the range in which the investigation was conducted.

5.323 Furnace Caps

Onto each of the two end pieces of the furnace, two caps were mounted to enclose the heating chamber.

The top cap consisted of a piece of brass rod 2 inches in length and 1 inch in diameter through which a 1/4 inch hole had been drilled. A set screw was mounted 1/4 of an inch from the top of the slug. Two additional holes 3/16 of an inch in diameter were also drilled through the slug to provide a means of inserting two thermocouples into the furnace chamber. The brass slug was brazed to a brass plate 2 inches square and 1/4 of an inch thick. The slug when mounted projected through the plate about 7/8 of an inch on each side. The brass plate was then used to mount the slug to an aluminum plate 8 inches long, 3 inches wide, and 1/8 of an inch thick which was in turn used to mount the cap to the top of the furnace. The cap when mounted projected into the furnace tube about 3/4 of an inch.

The bottom cap consisted of a piece of brass rod 1 inch in length and 1 inch in diameter through which a 3/8 inch diameter hole had been drilled. The hole was drilled this size so that the head of the pin vise could pass through it. The brass slug was mounted by means of two screws to an aluminum plate similar to the one described above through which a 3/8 inch diameter hole had also been drilled. A

second hole was then drilled through the aluminum plate and brass slug and a small copper tube inserted and soldered in place. This tube provided an inlet through which inert gas could be fed into the furnace chamber. The aluminum plate was then used to mount the bottom cap to the furnace. The cap when mounted projected into the furnace tube approximately 7/8 of an inch.

5.324 Pendulum

The pendulum was made up of two parts, the upper support element, and the lower support element and inertial crossmember. The upper support element consisted of a small pin vise 3 inches long pinned to a steel rod 2 feet long and 1/4 inch in diameter. It was held in place in the furnace by means of the set screw in the upper cap.

The lower support element consisted of a similar pin vise 3 inches long pinned to a steel rod 3/16 of an inch in diameter and 7 inches long. This rod in turn was pinned to a steel rod 1/4 inch in diameter and 4 inches long.

The inertial crosspiece consisted of a steel welding rod 1/8 of an inch in diameter and 20 inches long. It fitted through a hole drilled in the lower support element and was locked in place at its mid-point with a set screw. To the outer ends of the inertial crosspiece, an aluminum collar was slip fitted and six iron nuts were screwed onto each collar (Figure 10).

These iron nuts provided the additional weight for reducing the frequency of the inertial crossmember and also served as magnetic

material for the electromagnets to act upon. The pendulum was balanced by shifting the inertial crosspiece in the hole in the lower support element and locking it in place with the set screw.

A small mirror 1/2 inch long and 1/4 inch wide was glued to the lower support element. The mirror was used in conjunction with the lighting system to measure the amplitude of vibration of the pendulum. The total weight of the lower support element and inertial crossmember of the pendulum, including the mirror, was 113 grams. During operation, the bottom end of the lower support element of the pendulum was dipped into a beaker of oil to damp out any lateral vibrations of the pendulum.

As can be seen from Figure 8, the specimen formed part of the suspension element of the pendulum. The specimen was connected between the pin vises of the upper and lower support elements of the pendulum.

5.325 Electromagnet and Controls

An aluminum plate recessed on the front side for the lower support element was mounted 4 inches below the bottom of the furnace. Two supports were then attached to this plate so as to project out through the legs of the furnace support on both sides. An electromagnet was then attached to the end of each support. The supports were slotted so that the electromagnets could be adjusted so as to position them directly across from the iron nuts on each end of the inertial crossmember (Figure 10).

Oscillation of the pendulum was then induced by momentarily activating the electromagnets so that they attracted the iron nuts on the inertial crosspiece. The electromagnets were controlled by means of a toggle switch, the current being supplied by a small step-down transformer.

5.326 Light and Scale System

The same light and scale system described for Torsional Pendulum One was used except the size of the marker wire was changed. A marker wire .00125 inches in diameter was used for torsional measurements, and a marker wire .0035 inches in diameter was used for elastic-after effect measurements.

5.33 Modification of Torsional Pendulum Two for Elastic After-Effect Measurements

For elastic after-effect measurements, the inertial crossmember was removed from the lower support element of the pendulum, and in its place, a small aluminum collar was attached. A stiff wire 1/8 inch in diameter and 3 1/4 inches long was mounted to the front of the aluminum collar. To the bottom of the lower support element, another small aluminum collar was mounted with two small paddles attached to each side of it. During operation the paddles were submerged in oil and damped out any torsional vibrations when the lower support element was released during an elastic after-effect measurement.

A 1/4 inch diameter metal shaft, free to turn about its axis, was mounted between the two aluminum plates attached to the bottom of

the furnace. A metal support to which a protractor had been attached was then mounted to this shaft (Figure 11). By means of the support, the protractor could be adjusted in all three dimensions. A small adjustable stop was then mounted to the calibrated side of the protractor. Another small adjustable stop was mounted near the recessed slot in the bottom plate of the furnace.

The specimen could then be twisted through a small angle and held for the required period of time by adjusting the stop on the bottom plate of the furnace until it just touched the left side of the lower support element. The protractor was then adjusted until it was at the correct height and its center line centered on the lower support element. The small wire mounted on the collar described above was then turned to the left until it just engaged the stop mounted on the protractor. The stop mounted on the bottom plate of the furnace kept the lower support element centered while the specimen was being twisted. The specimen wire was released by simply rotating the protractor away from the lower support element of the pendulum which released the wire attached to the aluminum collar (Figure 12).

The same scale and lighting system described for the torsional measurements was used to measure the elastic after-effect. In this case, however, a longer scale and an increased distance between the mirror and scale were used.

5.4 Procedure

As stated at the beginning of Section 5, the procedure is described in two parts.

5.41 Section One, Pertaining to Torsional Pendulum One

5.411 Standardization of Thermocouple

Due to the unavailability of a thermocouple standardized by the National Bureau of Standards, the following check was made on the chromel-alumel thermocouple used in Torsional Pendulum One.

Time-temperature curves were run on three commercially pure metals Cd, Sn, and Zn. The true melting points of these metals are 320.9 C (Cd), 231.9 C (Sn), and 419.46 C (Zn) (28). The melting points of the three commercially pure metals determined from the time-temperature curves were 318 C (Cd), 233 C (Sn), and 423 C (Zn). While these variations did not provide an overall deviation from standard values, the check conducted did indicate that the thermocouple used was capable of temperature measurements within $\pm$ 3 1/2^{o}C.

5.412 Thermal Gradient in the Heating Chamber of Torsional Pendulum One

A check was made of the temperature uniformity obtainable in the heating chamber of Torsional Pendulum One. Since the greatest variation from uniformity could be expected at lower temperatures, observations at one inch intervals along the length of the tube were made in the range of 200 to 250^{o}C. Figure 13 shows the thermal gradient that was found to exist. The extent of this gradient was reduced by insertion of asbestos paper between the tube wall and tube clamps and by wrapping the tube ends, which projected outside the furnace, with asbestos cloth. The improved gradient is also shown in Figure 13.

While this condition did not assure the desired uniformity over the length of a specimen during an experimental run, unavailability of more precise equipment at the time of the early stage of the investigation necessitated its acceptance and resultant effects on the values obtained.

5.413 Typical Experimental Run Using Torsional Pendulum One

A sample of the experimental runs carried out on the various specimens is described as follows.

An 11 inch specimen of Alloy No. 1 (8.91 wt. percent AL) was cut from a bulk roll of wire. The wire was inserted in a porcelain tube and annealed in an electric muffle furnace for 30 hours at 700°C. This anneal served two purposes. The first and primary purpose was to remove the effects of cold work from prior drawing operations and to increase the grain size. The second purpose was to straighten the specimen.

The specimen was mounted in the torsional pendulum in the following manner. The lower cap of the heating chamber was unscrewed and removed. The upper support element of the pendulum was lowered to the bottom of the heating chamber by means of the counter-weight system. The top of the specimen was clamped in the upper pin vise. The bottom of the specimen was then attached to the pin vise of the lower support element so that a 10 inch distance was left between the tips of the pin vises. The lower support element of the pendulum was inserted through the hole in the lower cap which was then screwed to the bottom

of the furnace tube. This sequence of mounting was used because the head of the lower pin vise was larger than the hole through the lower cap. The upper support element, specimen, and lower support element of the pendulum were then raised into position by means of the counter weight system. The mirror and inertial crossmember were mounted on the lower support element at this time. The bottom of the lower support element was then placed in a small beaker of oil.

The specimen was annealed in place for two hours at 400°C. This anneal removed any cold work resulting from handling and mounting the specimen, and the weight of the lower support element and inertial crossmember served to finish the straightening of the specimen. With the specimen thus straightened and stabilized in position, the lower support element of the pendulum was centered in the hole in the lower cap of the heating chamber. Also at this time, the electromagnet was adjusted and centered behind the iron nuts on the right end of the inertial crossmember.

The light was turned on one hour prior to use. This precaution allowed the metal cup and marker wire to thermally stabilize, and thus prevented variations from the zero setting on the scale from occurring during operation due to thermal expansion.

A three-meter distance from the pendulum was measured and the scale positioned in the following manner. A peg with a three meter length of wire was mounted directly below the bottom of the lower support element of the pendulum. The scale was then positioned by adjusting it until the end of the three-meter wire would just touch

each end. The image of the marker wire was then focused and zeroed on the scale by adjusting the light.

The furnace was turned on and the heating chamber heated to the temperature at which that particular reading was to be made. One hour was allowed for the furnace to stabilize from one temperature setting to the next.

With the temperature stabilized, vibrations were excited in the pendulum by means of the electromagnet. When a sufficient amplitude of vibration was achieved, the forcing vibrations were stopped and the pendulum allowed to begin free decay. The pendulum was allowed to make several complete cycles before the scale readings were started, at which time the angle of oscillation was approximately 1 1/2 degrees. Depending on the damping, the number of vibrations between readings varied at different temperatures during the experimental run. All readings were taken on one side of the scale, and a reading consisted of recording the maximum point of deflection of the pendulum for that cycle. At critical points on the internal friction curve, two sets of readings were taken to insure that the points were reproducible. After a set of readings was taken, the temperature was re-checked to ascertain that it had not changed.

The internal friction was calculated and plotted for each set of readings while the furnace was heating up and stabilizing for the next set of readings. A sample calculation is given in Appendix A. Figure 14 shows the internal friction curve plotted from the data taken during this run.

Upon completion of the experimental run the specimen was removed from the pendulum and examined. The specimen showed a slight build-up of oxide on its surface from the run.

5.42 Section Two, Pertaining to Torsional Pendulum Two

The work described in this section was performed three years after that described in Section One.

5.421 Thermal Gradient in Torsional Pendulum Two

A check was made of the thermal gradient in the heating chamber of Torsional Pendulum Two in the following manner.

The center coil of the furnace was turned on and the temperature was adjusted by means of the variable transformer to the approximate temperature range in which the stress-induced ordering peak was expected. The end coils were then turned on, and, by means of the second variable transformer, the temperature was adjusted as closely as possible to that of the center section. After the temperature had stabilized, it was measured at 1 inch intervals along the length of the furnace tube. Figure 15 shows the thermal gradient that was found to exist. Two thermocouples were positioned within the furnace to monitor the temperature of specimen, one near its midpoint, and the other near its upper end.

5.422 Typical Experimental Run Using Torsional Pendulum Two

A sample experimental run carried out on the various specimen is described as follows: an 11 inch specimen of Alloy No. 1

(8.91 wt. per cent Al) was cut from the bulk roll of wire. As for Torsional Pendulum One, the wire again was inserted in a porcelain tube. However, the porcelain tube and specimen were sealed in a Vicor tube under an inert atmosphere of argon, and heated in a tube furnace for 50 hours at 700°C. As before, the purpose of this anneal was to remove the effects of prior cold work, to increase the grain size, and to straighten the specimen.

Upon removal from the tube furnace, the inside of the Vicor tube showed a very light stain of copper at the two ends. The tube was broken, and the specimen removed and etched lightly with ferric chloride. It was then mounted in the torsional pendulum in the following manner. The set screw in the top cap was loosened so that the upper pin vise could be lowered through the hole in the bottom cap by means of the upper pin vise. The top of the specimen was clamped in the upper pin vise, and the specimen partially raised up into the furnace. The bottom of the specimen was attached to the pin vise of the lower support element and inertial crossmember. The specimen was then fully raised into position, and the upper support element locked in place. The bottom of the lower support element was placed in a small beaker of oil.

The inert gas (nitrogen) was turned on, and the specimen was annealed in place for two hours at 400°C. This anneal served to remove any residual cold work imparted by handling and mounting the specimen, and afforded a further straightening effect. With the specimen thus straightened and stabilized in position, the lower support element was

centered in the hole in the lower cap of the heating chamber. Also at this time, the electromagnets were adjusted and centered behind the iron nuts on the ends of the inertial crossmember.

The light was turned on one hour prior to use for the same reasons as previously described in Section 5.413. The scale was positioned and the marker wire forcused as described in the same section.

The two variable transformers were turned on and the furnace heated to the particular temperature at which the reading was to be made. One hour was usually required to balance the temperatures in the end and center coils from one temperature to the next.

With the temperature stabilized, the pendulum was excited and the scale read in the same manner described in Section 5.413. Usually two sets of readings were taken at each point to check the reproducibility. After a set of readings were taken, the temperature was re-checked to ascertain that it had not changed.

The internal friction was calculated (as in Appendix A) and plotted (as in Figure 16) for each set of readings while the furnace was heating up and stabilizing for the next set of readings. Upon completion of each experimental run the specimen was removed from the pendulum and examined. Usually the surface of the specimen was dulled, indicating a slight build-up of oxide on its surface from the run.

5.423 Elastic After-Effect Measurement

The procedure used in carrying out the elastic after-effect measurements is described for a sample case as follows: a specimen

of Alloy No. 1 (8.91 wt. per cent Al) was prepared and mounted in the equipment in the same manner as described in Section 5.422.

The inert gas (nitrogen) was turned on, and the specimen annealed in place for 2 hours at 400°C. This anneal removed any cold work from handling and mounting the specimen, as well as finished straightening the specimen due to the weight of the lower support element. With the specimen thus straightened and stabilized in position, the lower support element was centered in the hole in the lower cap of the heating chamber. The furnace was then adjusted to a temperature of 340°C.

The metal stop mounted on the bottom aluminum plate of the furnace was adjusted against the left side of the specimen. The protractor was then adjusted into position and centered on the lower support element.

The specimen was twisted through an angle of approximately 6 degrees. The specimen was held in the twisted position for 6 hours and then was released by rotating the protractor away from the lower support element, releasing the wire attached to the collar. The paddles damped out the torsional vibrations in approximately 5 seconds. Zero time was taken from the moment the specimen was released.

The data then consisted of timing the marker wire as it passed down scale toward zero. The marker wire was timed for 33 minutes.

Typical data obtained from a run is tabulated in Table 4 and plotted in Figure 17. After approximately two hours, the marker wire was checked to ascertain whether it had returned to zero to insure that the specimen had not experienced a permanent set.

The specimen was then removed from the pendulum and examined.

6. RESULTS AND DISCUSSION

6.1 In General

The procedure described in Section 5.1 was only partially successful. The results obtained, both positive and negative, are summarized as follows:

a. Values of T_1, θ_1, and R_1 were found for Alloy No. 1, containing 8.91 w/o Al.

b. Values of T_1, θ_1, and R_1 were found for Alloy No. 2, containing 4.91 w/o Al.

c. Values of T_2 and R_2 were not found for either Alloy.

In accord with the notation adopted in Section 5, in which the Experimental Procedure was described in two stages, the Results and Discussion which follow are also presented in two parts.

6.2 Section One, Pertaining to Torsional Pendulum One

6.21 Identification of Stress-Induced Ordering Peaks (T_1,θ_1,R_1)

A series of tests were conducted to determine whether copper-aluminum alloys manifest a stress-induced ordering peak, and if so, to identify it.

Previous investigators have reported that the peak due to stress relaxation across grain boundaries is observed at approximately

the same temperature in the relaxation spectrum as the stress-induced ordering peak, and obscures it in fine-grained specimens. With an increase in grain size and consequently less grain boundary regions, less grain boundary relaxation occurs. The observed effect of this phenomenon is a displacement of the grain boundary relaxation peak to higher temperatures, resulting in less obscuring of the stress-induced ordering peak, which then becomes more clearly observable.

A series of three specimens of Alloy No. 1 (8.91 w/o Al) were given increasingly long anneals so that each succeeding specimen had a larger grain size than the previous one. The first specimen was annealed for 2 hours at 500°C, the second for 30 hours at 700°C, and the third for 50 hours at 700°C. Internal friction curves, (Figures 18, 14, and 19), were obtained for each, as described in Section 5.423. From the curves, it can be seen that the stress-induced ordering peak is most pronounced in Figure 19 at 392°C, corresponding to θ_1 of 9.71×10^{-3} and R_1 of .39 sec., although its presence is also suggested at the same temperature in Figures 14 and 18.

A comparable series of tests were not required for Alloy No. 2 (4.91 w/o Al) because the position on the temperature scale of its stress-induced ordering peak could be predicted from the position of the stress-induced ordering peak of Alloy No. 1. Figure 20 shows that the stress-induced ordering peak for Alloy No. 2 was obtained at 431°C, corresponding to θ_1 of 6.22×10^{-3} and R_1 of .39 sec., from a specimen annealed 50 hours at 700°C.

6.22 Reproducibility of Curves

An internal friction curve was re-run on the third specimen of Alloy No. 1 previously described above to determine whether any detectable change occurred in the specimen due to the previous experimental run. Figure 21 shows the internal friction curve that was obtained along with the original curve from the previous experimental run. The stress-induced ordering peak was found to occur at a temperature of 396°C. This value is 4° higher on the temperature scale than the previous peak, and, it occurred, as may be noted, at a lower value of internal friction.

This reduction in peak height and its shifting on the temperature scale is attributed to the slow oxidation of the surface of the specimen in the previous experimental run. A slight build-up of oxide was observed on the surface of the specimen after the first run, and this amount was observed to have increased after the second run. This condition indicated the need for an inert atmosphere to surround the specimen while at elevated temperatures, a practice which was incorporated in the design of Torsional Pendulum Two.

6.3 Section Two, Pertaining to Torsional Pendulum Two

6.31 Elastic After-Effect Measurements (T_2,R_2)

A series of elastic after-effect measurements were conducted on eight specimens, prepared as described in Section 5.423, over a temperature range varying from 250°C to 340°C. Figure 17 shows one

of the curves that was obtained from the specimen run at a temperature of 340°C. The slopes of the other curves obtained at lower temperatures were less steep indicating the temperature dependence of the elastic after-effect. None of the curves, however, showed the inflection point (Sketch B, Section 5.1) that was expected in alloys of this sort as described by Nowick (22).

According to Nowick, the elastic after-effect curve should show an inflection point if the grain size of the specimen is sufficiently large to minimize grain boundary relaxation effects. Such an inflection point should appear at that point on the curve which corresponds to the relaxation time for the particular specimen.

The absence of inflection points on the curves obtained for the copper-aluminum alloys suggested that either the apparatus was not sufficiently sensitive to detect them or that their grain size was not large enough.

To check these possibilities, two lines of action were pursued. First, the apparatus was applied to an elastic after-effect measurement of a specimen of the Cu-Zn system, Cu-15 a/o Zn, an alloy known to manifest stress-induced ordering and to display an inflection point on its elastic after-effect curve. Second, specimens of Alloy No. 1 (Cu-8.91 w/o Al) were given extensive anneals to produce in them the largest possible grain size.

6.32 Elastic After-Effect in Cu-15 a/o Zn

A Cu-Zn wire specimen containing 15 a/o Zn, and similar in all other respects to the Cu-Al specimens, was annealed for 48 hours at

750°C while sealed in a Vicor tube filled with Argon. An elastic after-effect measurement was run on this specimen at a temperature of 260°C. Figure 25 shows the curve that was obtained in which an inflection point appears at a time value, R, of 630 seconds.

This result was felt to be confirmation of the fact that the apparatus was sufficiently sensitive to provide the type of data desired and gave further indication that the grain size in the previously run specimens of Cu-Al was not large enough.

6.33 Annealing Treatments for Enlargement of Grain Size

The specimen for which the most pronounced stress-induced ordering peak had been recorded (Section 6.21 and Figure 19) also had a well-developed grain size. Figure 22 shows grains whose diameters are more than half the diameter of the wire. This specimen had been previously annealed for 50 hours at 700°C.

In an effort to reproduce this favorable grain structure, the same treatment was given to another specimen of Alloy No. 1. While a comparably large grain size did not result, a torsional measurement was nevertheless conducted on this specimen. It was desired to compare the curve obtained (Figure 16) with the curve previously obtained for a like specimen of larger grain size (Figure 19). Though the peak obtained in the latter was not duplicated, a suggestion of a peak is plainly visible in the smaller-grained specimen, further emphasizing the need for large-grained specimens in this type of measurement.

An extension of the annealing time to 70 hours at 700°C also failed to produce a noticeable grain enlargement.

Since 700°C was the safe upper annealing limit for retention of a single phase in Alloy No. 1, further anneals for obtaining large-grained samples were conducted on Alloy No. 2. The following annealing cycles were given:

24 hours at 850°C

50 hours at 850°C

6 hours at 950°C

24 hours at 950°C

While these anneals served to increase the grain sizes of the respective samples, only in the last treatment did they reach the proportions previously observed in Figure 22. While this treatment produced a well-developed grain size, it also resulted in a noticeable deterioration of the specimen. Considerable leaching of aluminum appeared to have resulted along the surface of the specimen and microexamination showed cracks in its core. This condition was not surprising in view of the proximity of the annealing temperature to the melting point for that composition.

Notwithstanding the unfavorable condition of the specimen, however, a torsional measurement was conducted to determine whether the enlarged grain size would duplicate the prior peak obtained for Alloy No. 2 (Figure 20). The observations, however, were quite erratic and did not justify further consideration (Figure 23).

6.4 Summary

The experimental work heretofore described, has not achieved the full measure of positive results which were sought at the outset of the investigation. It has shown, however, that the alloys considered do exhibit the stress-induced ordering effect. The inability to relate this effect to temperature does not appear to be caused by the functioning of the apparatus used but rather seems to be attributable to the nature of the material from which the wire specimens were made. The wire itself was obtained from a commercial source and its chemical analysis shows the presence of impurities in larger amounts than desirable. While at the start of the investigation, the magnitude of the impurities were not thought to be of great significance, it has subsequently appeared to be responsible for inhibiting the grain enlargement which is so essential in this type of work.

The investigation as conducted has shown every indication of producing the objective originally sought. It is felt, therefore, that further effort along the same lines is justified if specimens of higher purity are employed.

7. CONCLUSIONS

From the results obtained in this investigation the following conclusions may be drawn:

1. A copper-aluminum alloy containing 4.91 w/o aluminum exhibits a stress-induced ordering peak at 431°C, as measured by torsional damping at a frequency of .41 cycles per second.
2. A copper-aluminum alloy containing 8.91 w/o aluminum exhibits a stress-induced ordering peak at 392°C as measured by torsional damping at a frequency of .41 cycles per second.

BIBLIOGRAPHY

1. Nowick, A. S., "Internal Friction in Metal," Progress in Metal Physics, Vol. 4, Interscience Publishers, Inc., New York, 1953, p. 1.

2. Zener, C., Elasticity and Anelasticity of Metals, The University of Chicago Press, Chicago, 1956.

3. Snoek, J. L., "Mechanical After Effect and Chemical Constitution," Physica, Vol. 6, July 1939, p. 591.

4. Snoek, J. L., "Effect of Small Quantities of Carbon and Nitrogen on the Elastic and Plastic Properties," Physica, Vol. 8, July 1941, p. 711.

5. Dijkstra, L. J., "Elastic Relaxation and Some Properties of the Solution of Carbon and Nitrogen in Iron," Philips Research Reports, No. II, 1947, p. 357.

6. Ke, T. S. and Ma, Y. L., "Internal Friction Peak Associated With the Stress-Induced Diffusion of Carbon in Low Carbon Alloy Martensite," Scienta Sinica, Vol. 6, February 1957, p. 81.

7. Ke, T. S. and Tsien, C. T., "On the Mechanism of the Internal Friction Peaks Associated With the Stress-Induced Diffusion of Carbon in Face-Centered Cubic Alloy Steels," Scienta Sinica, Vol. 5, December 1956, p. 625.

8. Zener, C., "Internal Friction of a Alpha-Brass Crystal," Trans. of the AIME, Vol. 152, Inst. of Mining and Metallurgical Engineers, Inc., New York, 1943, p. 122.

9. Zener, C., "Stress Induced Preferential Orientation of Pairs of Solute Atoms in Metallic Solid Solutions," Physical Review, Vol. 71, January 1947, p. 34.

10. Nowick, A. S., "Resonance and Relaxation Phenomena," Resonance and Relaxation in Metals, ASM, 1961, p. I-21.

11. Berry, B. S., "Magnitude of the Zener Relaxation Effect, Pt. IV Anisotropy of the Relaxation Strength in Al-4 Per Cent Cu," Acta Met., Vol. 9, February 1961, p. 98.

12. Le Clare, A. D. and Lomer, W. M., "Relaxation Effects in Solid Solutions Arising from Changes in Local Order, Pt. II Theory of the Relaxation Strength," Acta Met., Vol. 2, November 1954, p. 742.

13. Seraphim, D. P. and Nowick, A. S., "Magnitude of the Zener Relaxation Effect, Pt. III Anisotropy of the Relaxation Strength in Ag-Zn and Li-Mg Solid Solutions," Acta Met., Vol. 9, February 1961, p. 85.

14. Artman, R. A., "Temperature Dependence of Young's Modulus and Internal Friction of Single Crystals of Beta-Brass," J. of Applied Phys., Vol. 23, April 1952, p. 475.

15. Hino, C., Tomizuka, C., and Wert, C., "Internal Friction and Diffusion in 31 Per Cent Alpha-Brass," Acta Met., Vol. 5, January 1957, p. 42.

16. Le Clare, A. D., "Diffusion in Metals," Progress in Metal Physics, Vol. 4, Interscience Publishers, New York, 1953, p. 320.

17. Wert, C., "Measurement on the Diffusion of Interstitial Atoms in B.C.C. Lattices," J. of Applied Phys., Vol. 21, November 1950, p. 1196.

18. Wert, C., "Diffusion Coefficient of C in Alpha-Iron," Physical Review, Vol. 79, October 1950, p. 601.

19. Wert, C. and Zener, C., "Interstitial Atomic Diffusion Coefficients," Physical Review, Vol. 76, October 1949, p. 1169.

20. Stanley, J. and Wert, C., "Anelastic Measurements of Diffusion Coefficients," Resonance and Relaxation in Metals, ASM, 1961, p. x-6.

21. Lazarus, D. and Tomizuka, C., "Self-Diffusion, in Silver-Zinc," Physical Review, Vol. 103, September 1956, p. 1155.

22. Nowick, A. S., "Anelastic Measurements of Atomic Mobility in Substitutional Solid Solutions," Physical Review, Vol. 88, November 1952, p. 925.

23. Turner, T. J. and Williams, G. B., "Internal Friction in Silver Solid Solutions," Acta Met., Vol. 10, April 1962, p. 305.

24. Bardeen, J. and Herring, C., "Diffusion in Alloys and the Kirkendall Effect," Imperfections in Nearly Perfect Crystals, John Wiley and Sons, Inc., New York, 1952, p. 261.

25. Kuper, A., Lazarus, D., Manning, J., and Tomizuka, C., "Diffusion in Ordered and Disordered Copper-Zinc," Physical Review, Vol. 104, December 1956, p. 1536.

26. Timoshenko, S. and Mac Cullough, G. H., Elements of Strength of Material, D. Van Nostrand, Co., New York, 1955.

27. Ke, T. S., "Experimental Evidence of the Viscous Behavior of Grain Boundaries in Metals," Physical Review, Vol. 71, April 1947, p. 533.

28. Metals Handbook, American Society of Metals, 1948.

APPENDIX A

A SAMPLE INTERNAL FRICTION CALCULATION

The following scale readings were taken during an experimental run on a specimen of Alloy No. 1 (8.91 w/o Al) annealed at 700°C for 30 hours. The scale readings were: 7.45 - 4 intervening cycles - 7.25 - 4 intervening cycles - 7.05 - 4 intervening cycles - 6.85 - 4 intervening cycles - 6.65. The furnace temperature was 279.5 C.

Figure 24 shows these scale readings plotted on semi-log paper, and as can be seen, the points form a straight line. d, the ratio of the amplitudes of vibration in free decay must equal the slope of the above line. Therefore, the following equation may be written for d.

$$d = \frac{1}{n} \ln \frac{x_o}{x_n}$$

where x_o is the initial scale reading, and n is the number of cycles of the pendulum required to reduce this value to the scale reading x_n.

Substituting the first and last scale readings into the above equation gives (see Table 3):

$$d = \frac{1}{20} \ln \frac{7.45}{6.65} = \frac{1}{20}(2.00821 - 1.89462) = \frac{1}{20} \ (.11359) = .005679$$

Substituting the value found for d into Equation 25 (Section 4.1), the value of the internal friction θ was calculated as

$$\theta = \frac{d}{\pi} = \frac{.005679}{3.14} = .00181$$

TABLE 1

SOME VALUES OF D_o AND ΔH DETERMINED BY ANELASTIC METHODS FOR DIFFUSION OF CARBON, NITROGEN, AND OXYGEN IN DILUTE B. C. C. INTERSTITIAL ALLOYS (20)

Alloy	D_o sq cm per sec	ΔH cal per mole
C in Fe	0.02	20,100
N in Fe	0.003	18,200
C in Ta	0.006	38,500
N in Ta	0.006	33,000
O in Ta	0.004	25,500
C in Cb	0.004	33,000
N in Cb	0.009	34,900
O in Cb	0.02	26,900
C in V	0.005	27,300
N in V	0.009	34,000
O in V	0.01	29,000

TABLE 2

COMPOSITION OF ALUMINUM BRONZES

Element	Alloy 2 wt. Per Cent	Alloy 1 wt. Per Cent
Ag	< .005	-
Al	4.91	8.91
As	N. D.	N. D.
Bi	N. D.	N. D.
Cu	94.96	91.04
Fe	.02	.03
Mn	< .005	< .01
Ni	< .005	< .005
Sb	N. D.	N. D.
Si	.04	< .01
Sn	< .001	< .005
P	N. D.	N. D.
Pb	< .01	< .005
Zn	N. D.	< .05

TABLE 3

SAMPLE EXPERIMENTAL DATA FOR A TORSIONAL MEASUREMENT

Composition of Specimen:	8.91 wt. Per Cent Al
Annealing Temperature:	700°C
Annealing Time:	30 Hours
Frequency of Pendulum:	.409 cps
Equipment:	Torsional Pendulum One

Temperature C	Scale Reading x	n - 1	ln x	d	θ
	7.225		1.97754		
265.5	6.55	19	1.87947	.00490	.00156
	7.275		1.98444		
272	6.75	14	1.90954	.00432	.00139
	7.45		2.00821		
279.5	6.65	19	1.89462	.00568	.00181
	7.45		2.00821		
287.5	6.70	19	1.90211	.00530	.00169
	7.35		1.99470		
296.5	6.525	19	1.87564	.00595	.00189
	7.45		2.00821		
302	6.40	24	1.85630	.00608	.00194
	7.30		1.98787		
312	6.15	25	1.81645	.00659	.00210
	7.25		1.98100		
321	6.325	19	1.84451	.00682	.00217
	7.25		1.98100		
328.5	6.30	19	1.84055	.00702	.00224
	7.45		2.00821		
336	6.30	20	1.84055	.00800	.00255
	7.45		2.00821		
343	6.30	20	1.84055	.00800	.00255
	7.45		2.00821		
352	5.85	20	1.76644	.01150	.00366
	7.20		1.97408		
357	5.425	19	1.69102	.01415	.00451
	7.10		1.96009		
367	5.50	11	1.70475	.02128	.00678
	7.45		2.00821		
374	6.10	8	1.80829	.02221	.00707
	7.45		2.00821		
380	5.80	9	1.75786	.02504	.00797
	7.45		2.00821		
389.5	6.00	7	1.79176	.02705	.00861

TABLE 3 (Continued)

	7.45		2.00821		
398	6.25	5	1.83258	.02927	.00932
	7.25		1.98100		
408	5.05	11	1.61939	.03014	.00960
	7.55		2.02155		
416	4.65	13	1.53687	.03462	.01102
	7.75		2.04769		
424	4.55	13	1.51513	.03804	.01211
	7.55		2.02155		
430	4.25	13	1.44692	.04104	.01307
	7.00		1.94591		
440	4.45	9	1.49290	.04530	.01442
	7.40		2.00148		
451	4.375	9	1.47590	.05256	.01674
	7.75		2.04769		
	4.60	9	1.52606	.05216	.01661
	7.20		1.97408		
458	3.90	9	1.36098	.06131	.01952
	7.35		1.99470		
	3.95	9	1.37372	.06210	.01977
	7.65		2.03471		
462.5	4.025	9	1.39252	.06422	.02045
	7.30		1.98787		
	3.825	9	1.34155	.06463	.02058
	7.20		1.97408		
471.5	3.80	9	1.33500	.06391	.02035
	7.45		2.00821		
	3.925	9	1.36736	.06409	.02040
	7.00		1.94591		
475.5	4.35	7	1.47018	.05946	.01893
	7.25		1.98100		
	4.55	7	1.51513	.05823	.01854
	7.05		1.95303		
486.5	4.15	7	1.42311	.06624	.02109
	7.25		1.98100		
494	5.55	2	1.71380	.08906	.02836

TABLE 4

SAMPLE EXPERIMENTAL DATA FOR AN
ELASTIC AFTER-EFFECT MEASUREMENT

Composition of Specimen:	8.91 wt. Per Cent Al
Annealing Temperature:	700°C
Annealing Time:	50 Hours
Time Twisted:	6 Hours
Angle Twisted:	Approximately 6 Degrees
Temperature of Measurement:	340°C

Scale Reading	Time, Seconds	Scale Reading	Time, Seconds
7.2	15	4.3	525
7.0	20	4.2	563
6.8	33	4.1	614
6.6	47	4.0	672
6.4	61	3.9	728
6.2	80	3.8	778
6.1	92	3.7	782
6.0	105	3.6	840
5.9	115	3.5	977
5.8	130	3.4	1035
5.7	148	3.3	1103
5.6	163	3.2	1166
5.5	180	3.1	1245
5.2	240	3.0	1325
5.1	257	2.9	1405
5.0	295	2.8	1480
4.9	321	2.7	1614
4.8	344	2.6	1658
4.7	376	2.5	1772
4.6	405	2.4	1867
4.5	440	2.3	2006
4.4	475		

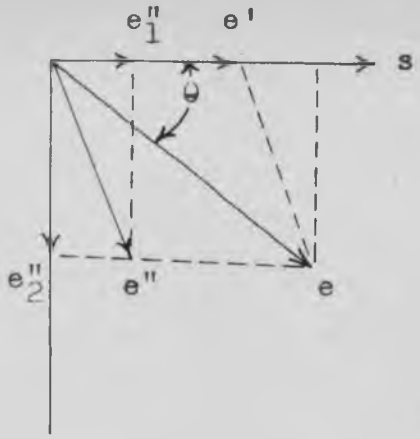

Figure 1

Vector Diagram of the Phase Relationship between Stress and Strain (1).

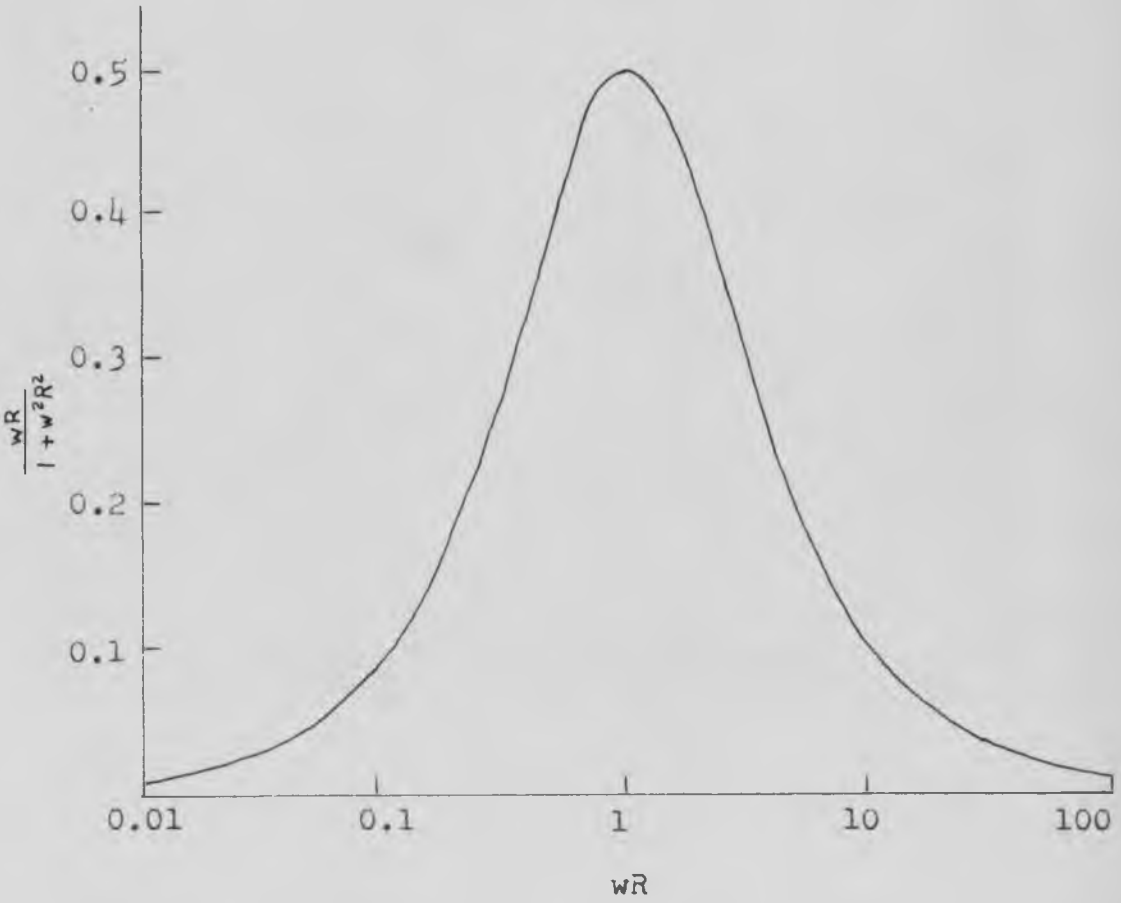

Figure 2

Plot of the Factor $\frac{wR}{1 + w^2R^2}$ against ln wR.

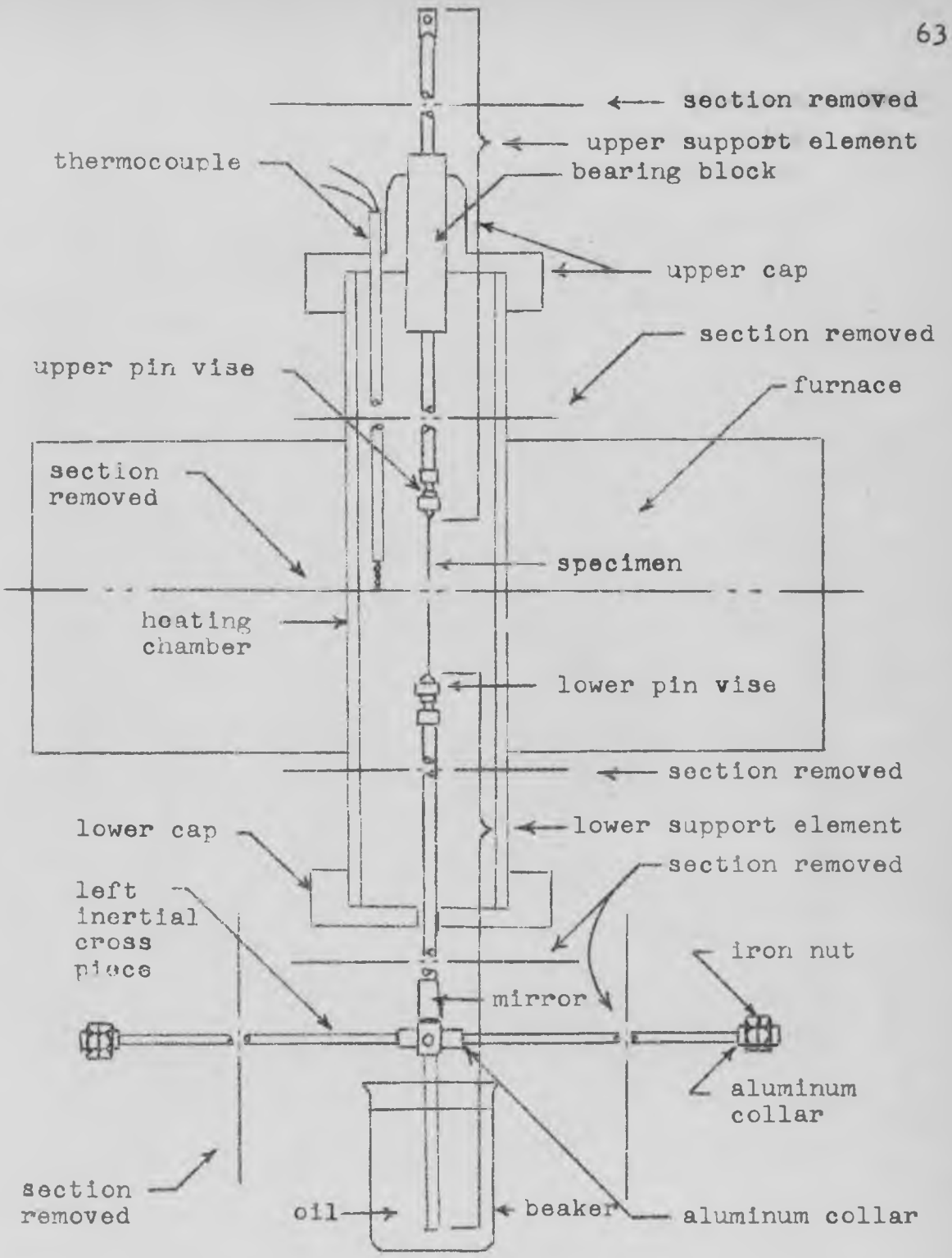

Figure 3

Schematic Diagram of Torsional Pendulum One

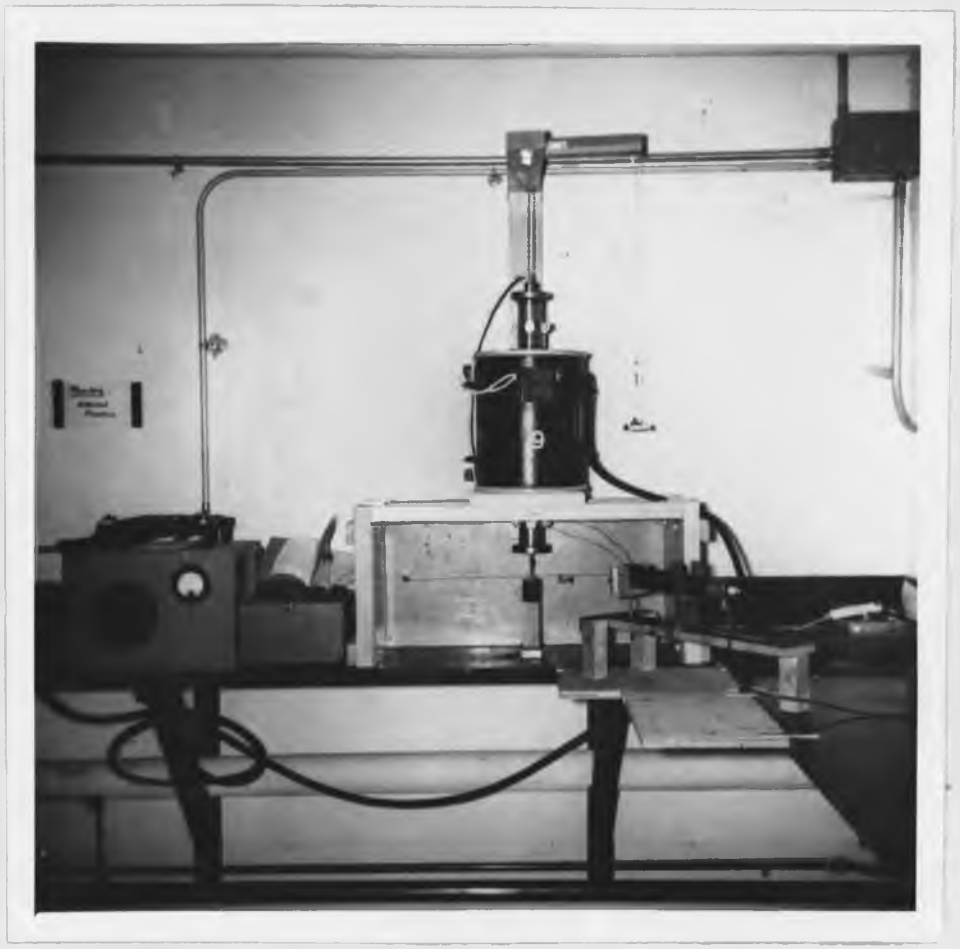

Figure 4

Front View of Torsional Pendulum One.

Figure 5

Front View of Inertial Crossmember, Mirror, and Electromagnet of Torsional Pendulum One.

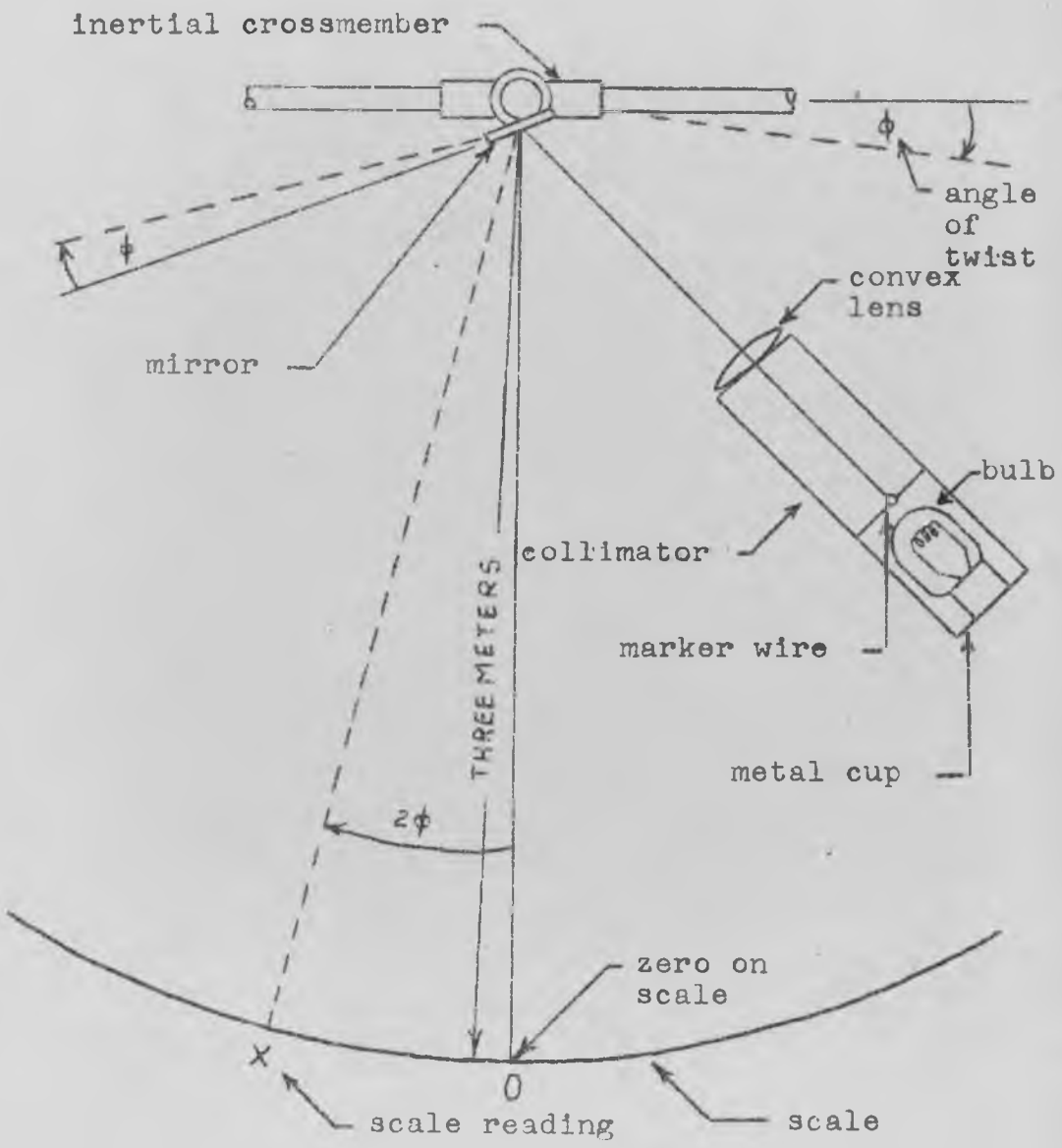

Figure 6

Schematic Drawing of Light and Scale System.

Figure 7

Side View of Scale

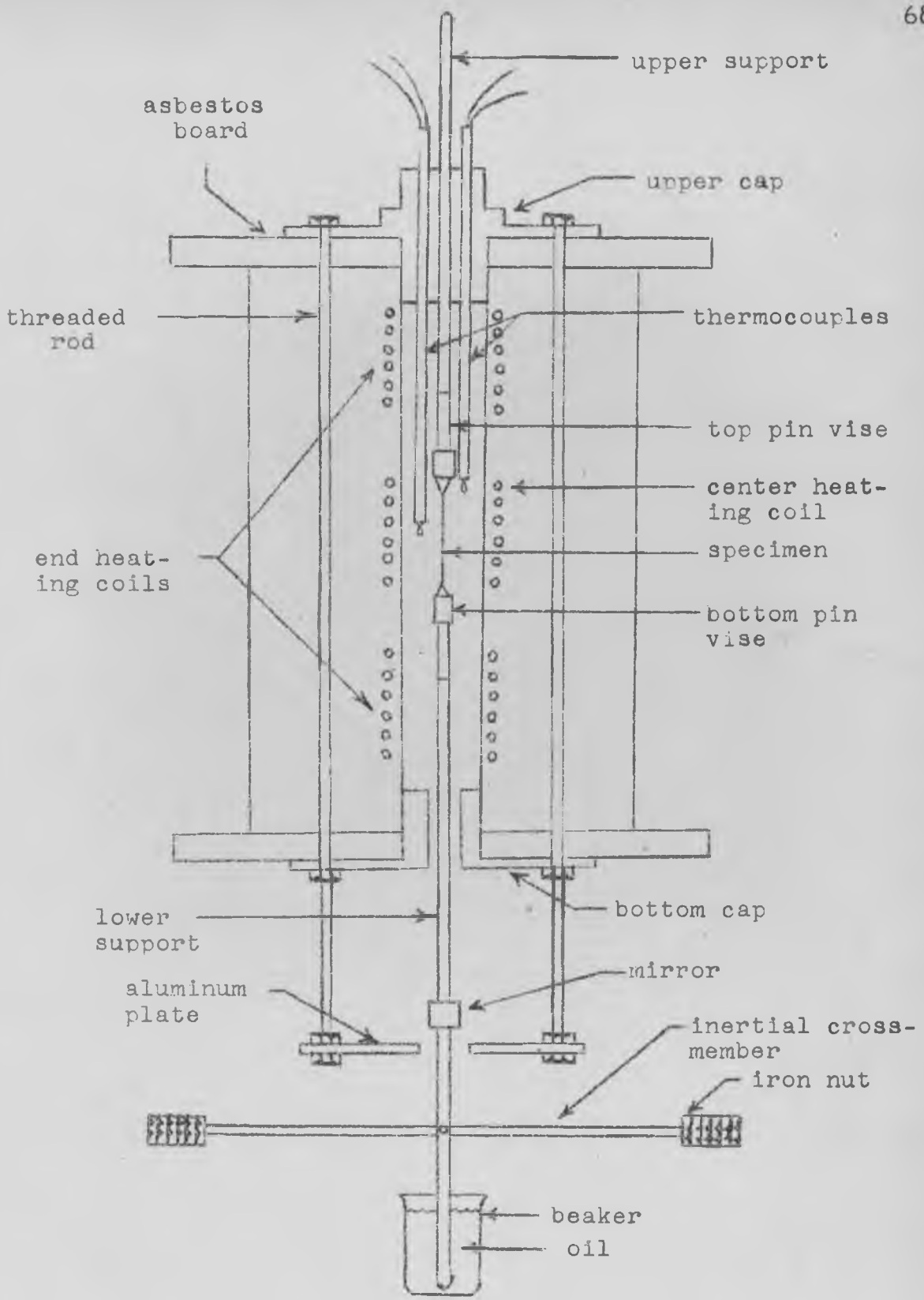

Figure 8

Schematic Diagram of Torsional Pendulum Two.

Figure 9

Front View of Torsional Pendulum Two.

Figure 10

Front View of Inertial Crossmember, Mirror, and Electromagnets of Torsional Pendulum Two.

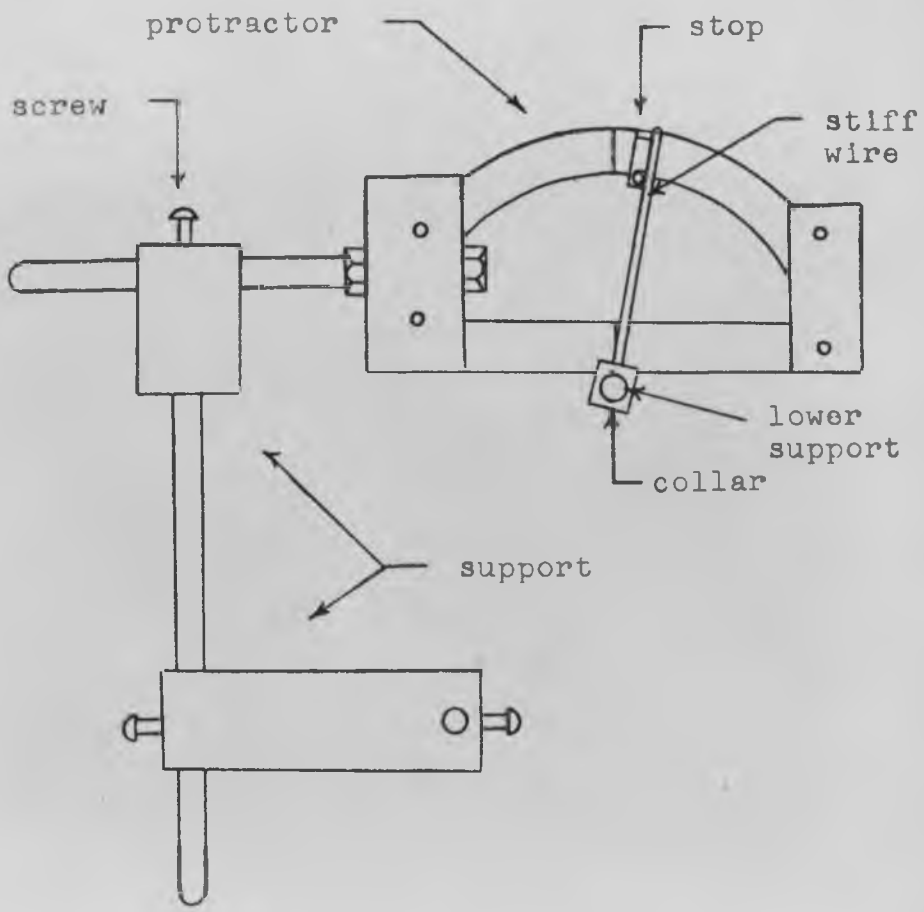

Figure 11

Schematic Diagram of Method Used to Twist Specimen for an Elastic After-Effect Measurement.

Figure 12

Front View of Furnace Modified for
Elastic After-Effect Measurements.

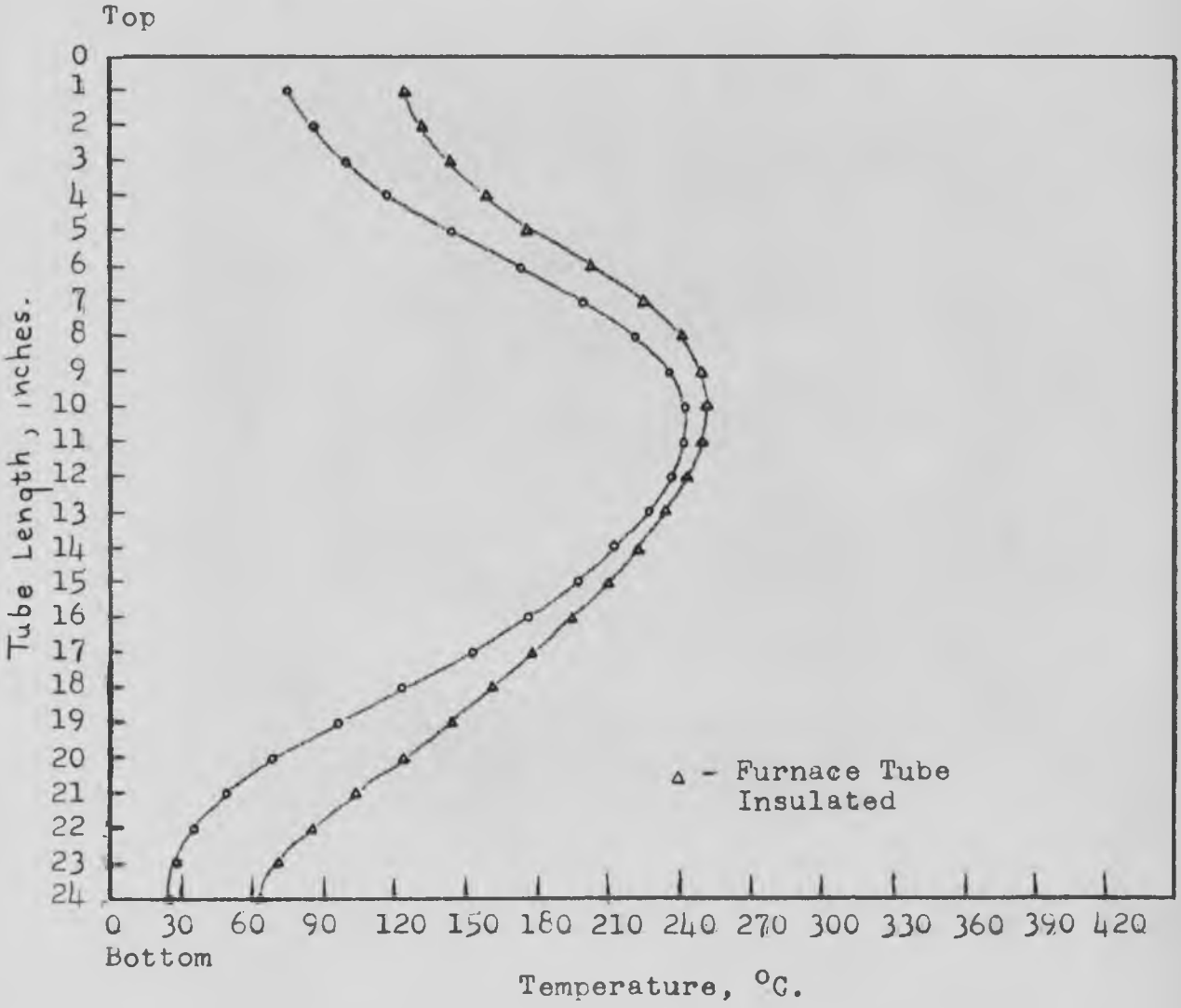

Figure 13

Thermal Gradient in Heating Chamber of Torsional Pendulum One.

Figure 14

Internal Friction Curve of a Specimen (Cu-8.91 w/o Al) Annealed 30 Hours at 700°C (Torsional Pendulum One).

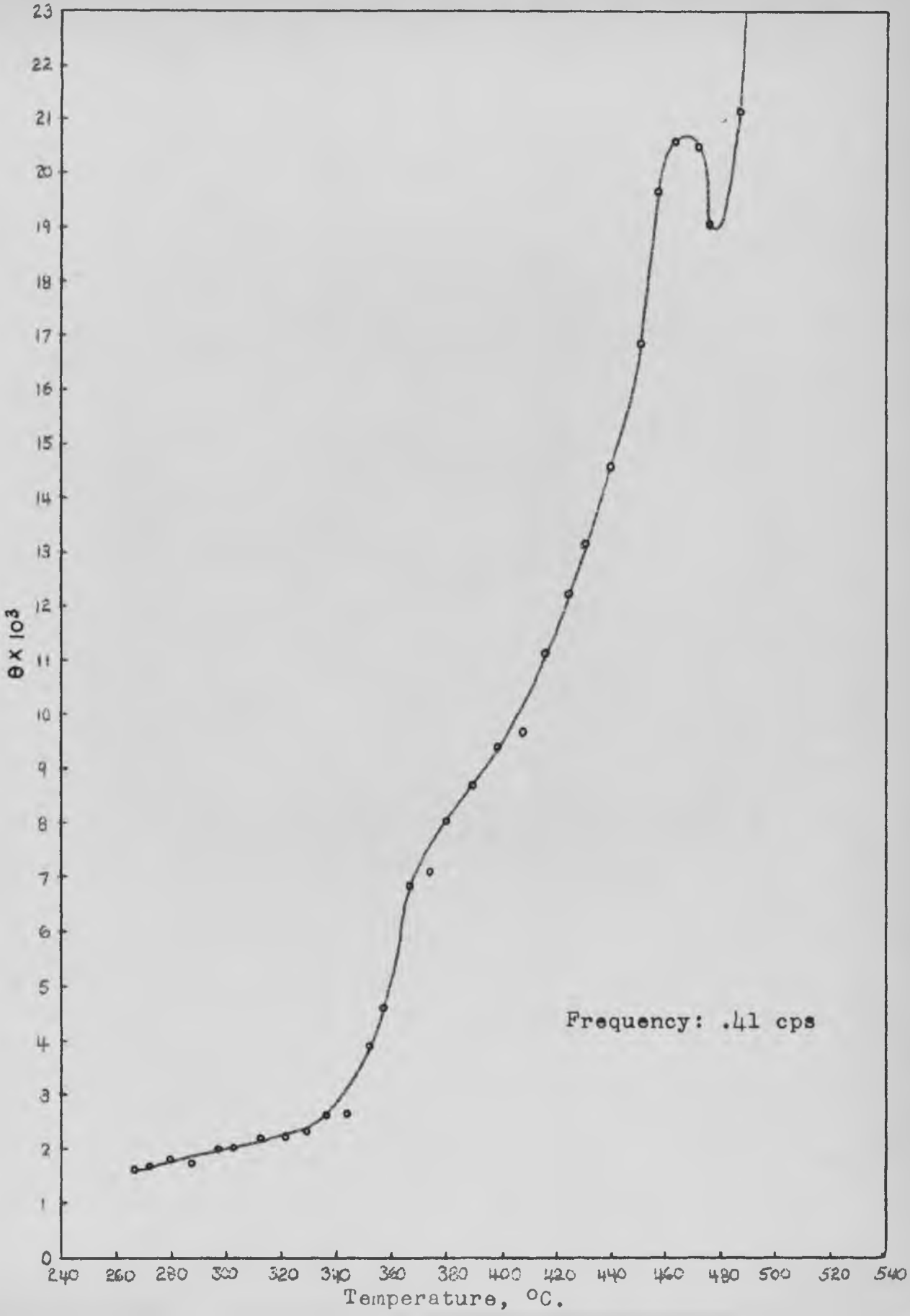
θ X 10³
0
1
2
3
4
5
6
7
8
9
10
11
12
13
14
15
16
17
18
19
20
21
22
23
240
260
280
300
320
340
360
380
400
420
440
460
480
500
520
540
Temperature, °C.
Frequency: .41 cps

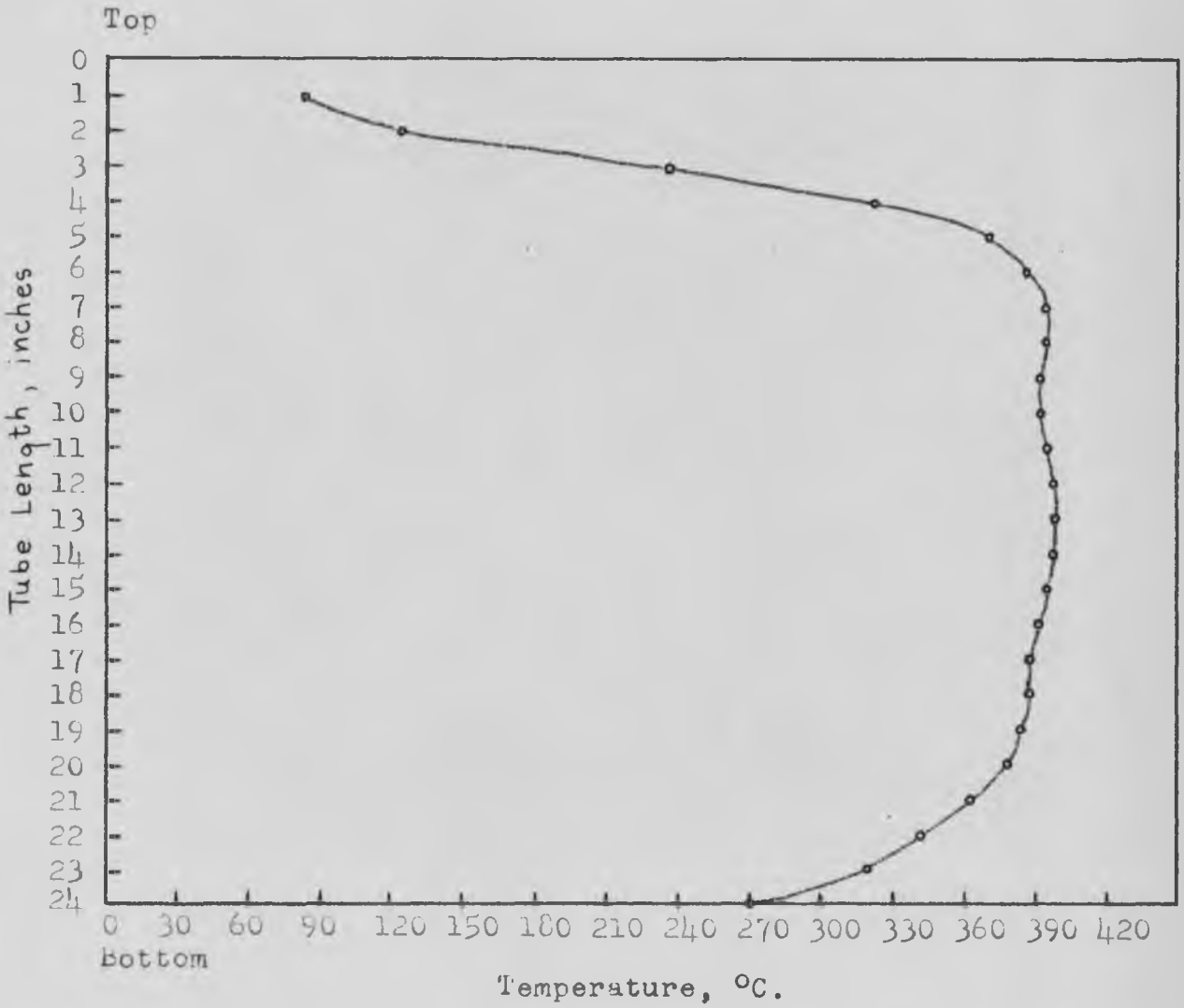

Figure 15

Thermal Gradient in Heating Chamber
of Torsional Pendulum Two.

Figure 16

Internal Friction Curve of a Specimen (Cu-8.91 w/o Al) Annealed 50 Hours at 700°C (Torsional Pendulum Two).

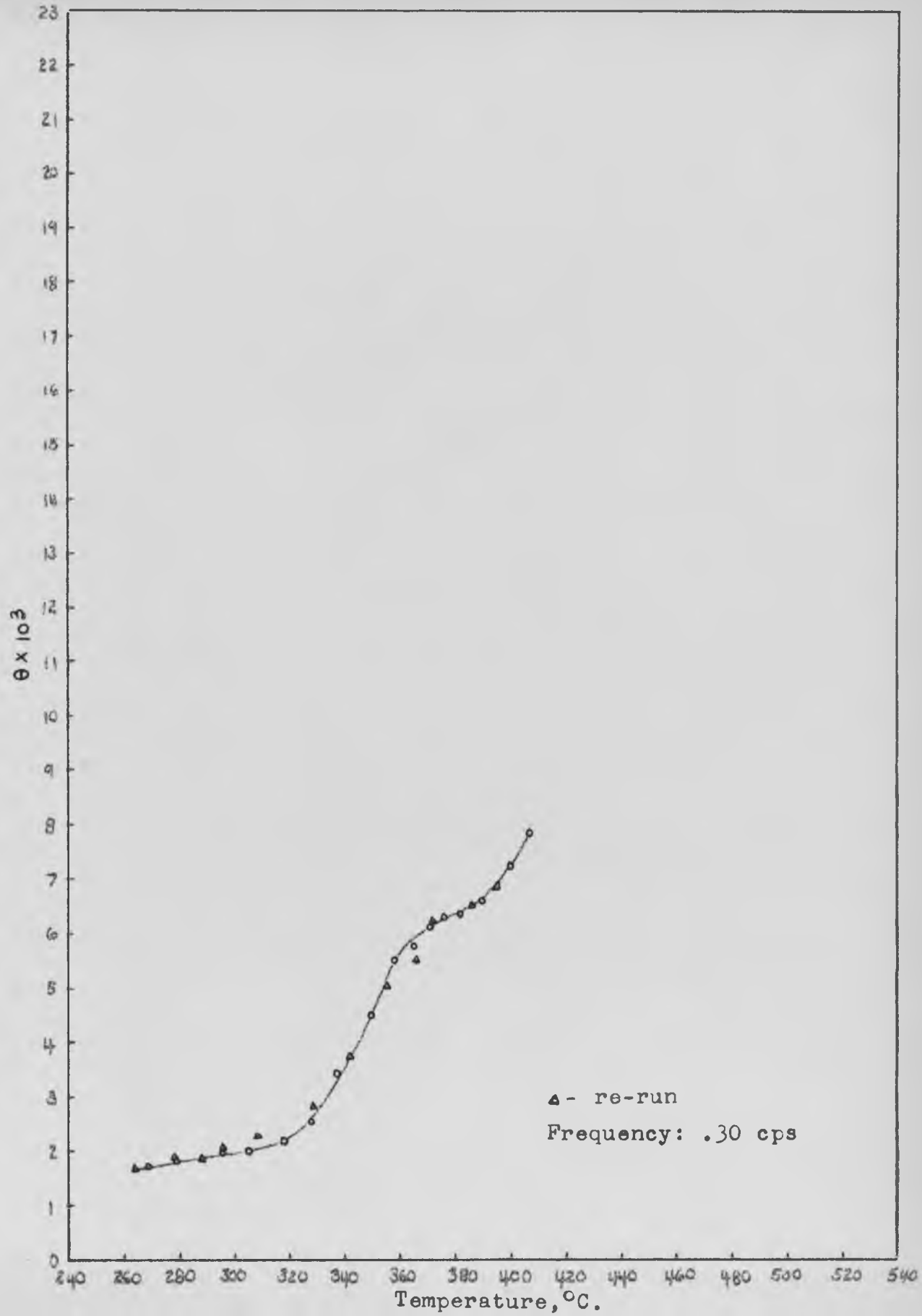
θ x 10³
Temperature, °C.
▲- re-run
Frequency: .30 cps

Figure 17

Elastic After-Effect Curve of a Specimen (Cu-8.91 w/o Al) (Annealed 50 Hours at 700°C) Measured at 340°C.

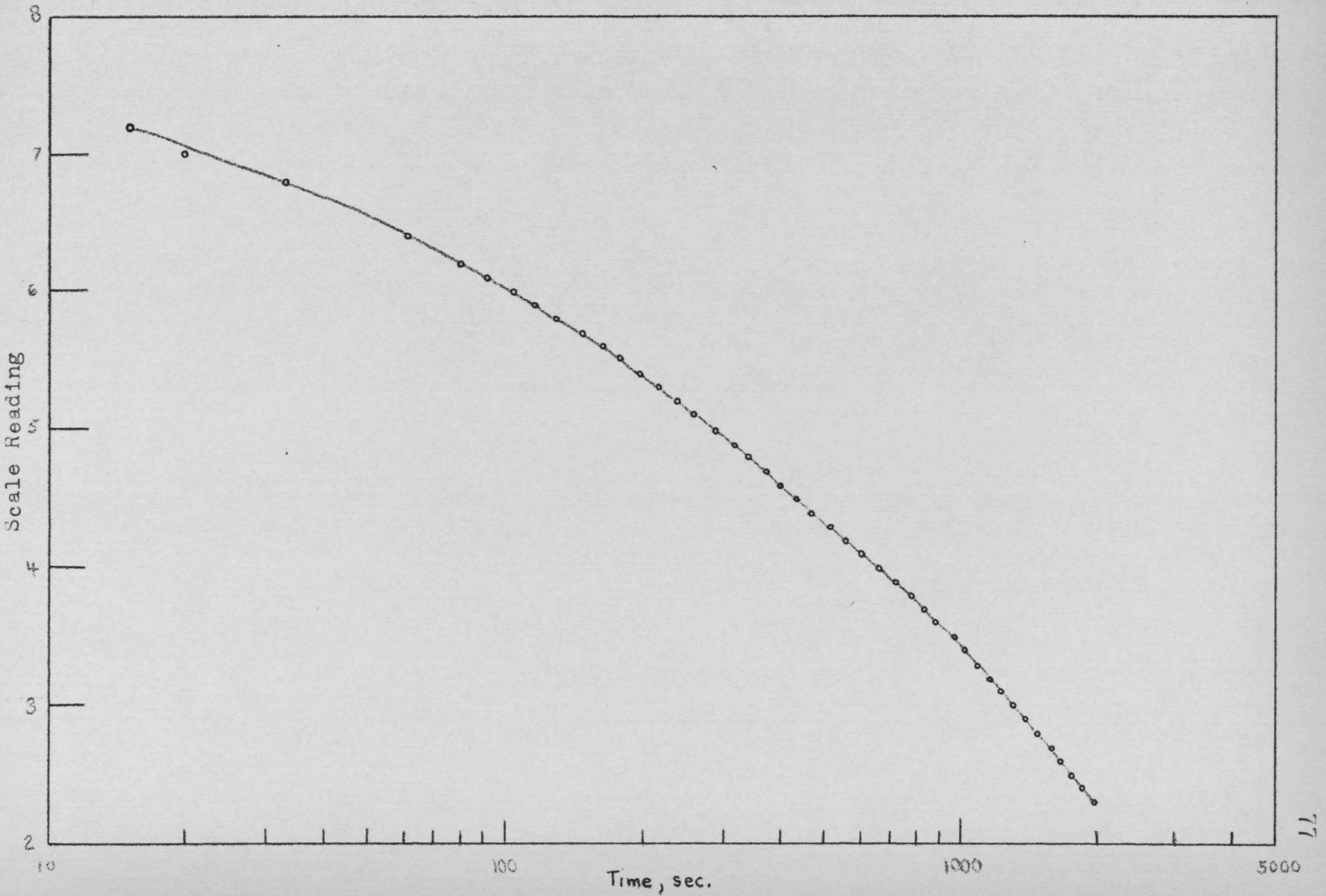
8
7
6
5
4
3
2
Scale Reading
10
100
1000
5000
Time, sec.

Figure 18

Internal Friction Curve of a Specimen (Cu-8.91 w/o Al) Annealed 2 Hours at 500°C (Torsional Pendulum One).

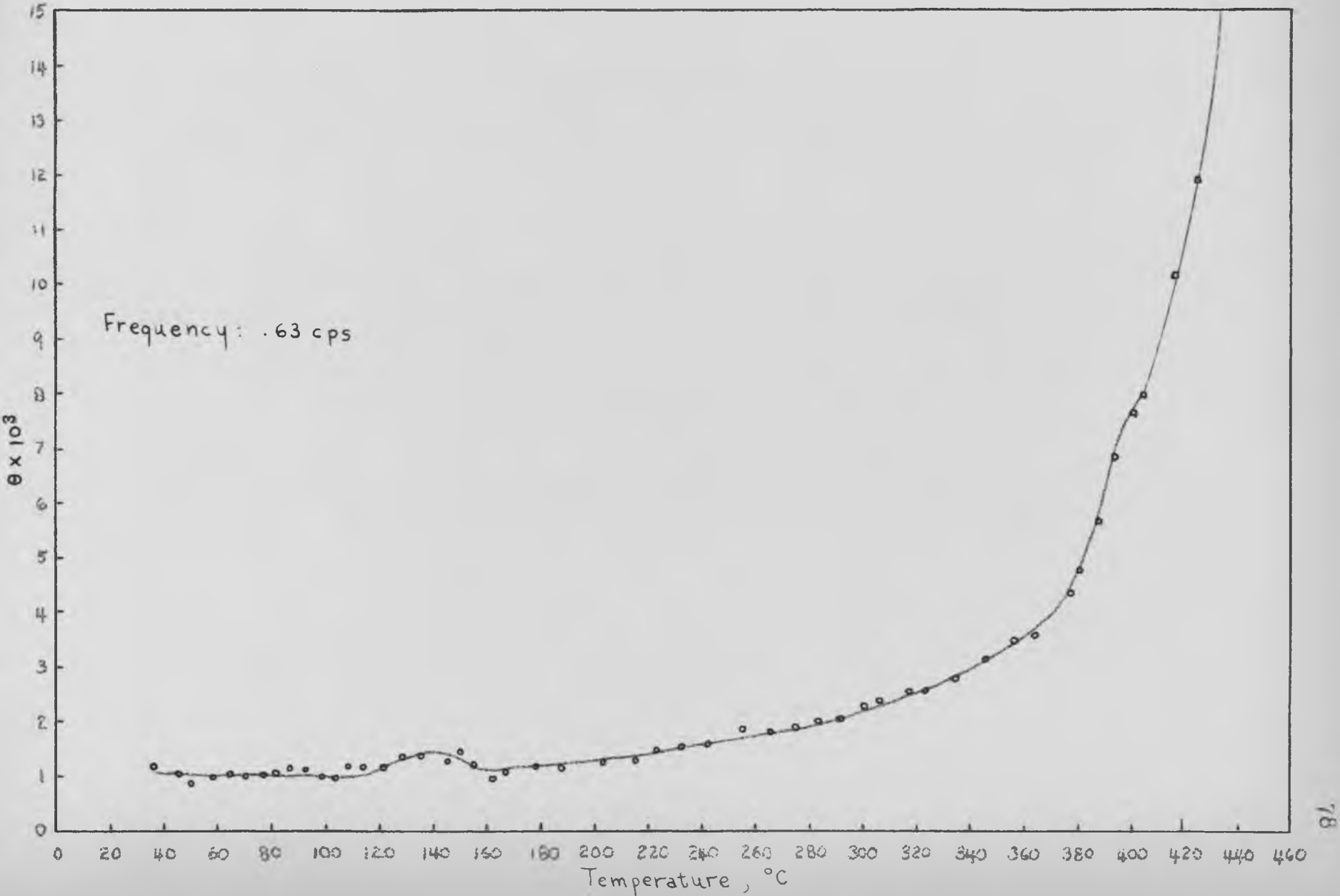
Frequency: .63 cps
θ x 10³
Temperature, °C
0
1
2
3
4
5
6
7
8
9
10
11
12
13
14
15
0
20
40
60
80
100
120
140
160
180
200
220
240
260
280
300
320
340
360
380
400
420
440
460

Figure 19

Internal Friction Curve of a Specimen (Cu-8.91 w/o Al) Annealed 50 Hours at 700°C (Torsional Pendulum One).

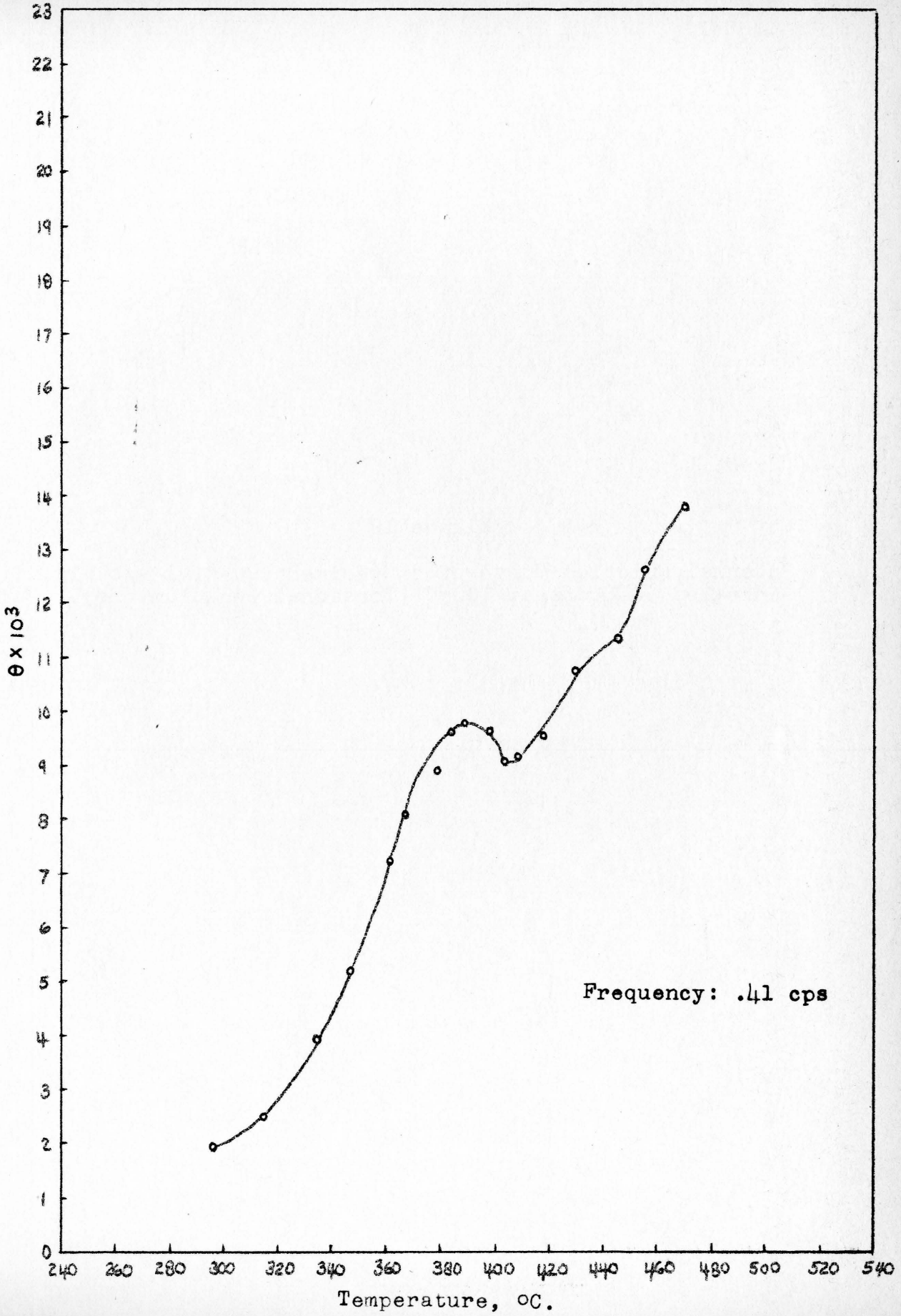
θ X 10³
0
1
2
3
4
5
6
7
8
9
10
11
12
13
14
15
16
17
18
19
20
21
22
23
240
260
280
300
320
340
360
380
400
420
440
460
480
500
520
540
Temperature, °C.
Frequency: .41 cps

Figure 20

Internal Friction Curve of a Specimen (Cu-4.91 w/o Al) Annealed 50 Hours at 700°C (Torsional Pendulum One).

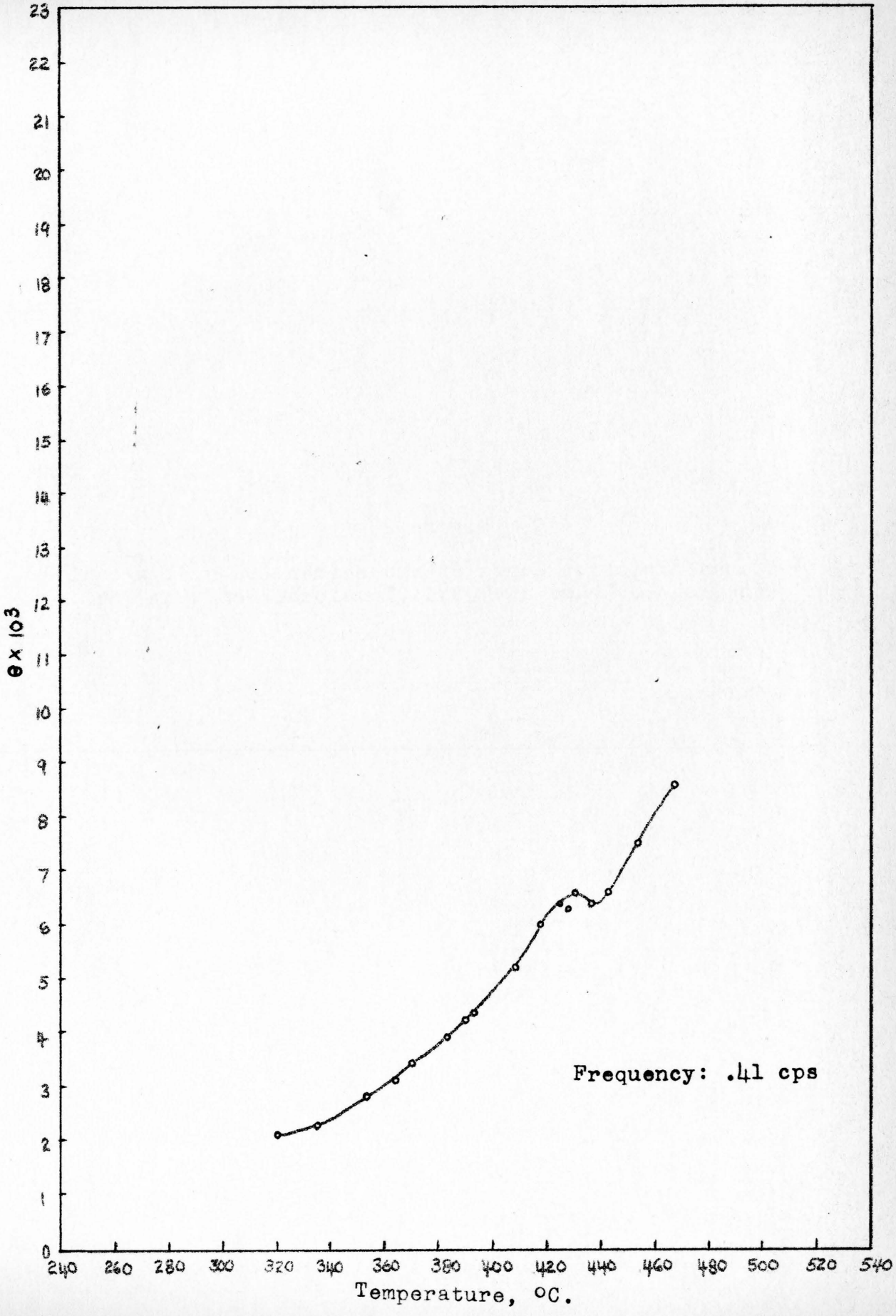
θ x 103
0
1
2
3
4
5
6
7
8
9
10
11
12
13
14
15
16
17
18
19
20
21
22
23
240
260
280
300
320
340
360
380
400
420
440
460
480
500
520
540
Temperature, °C.
Frequency: .41 cps

Figure 21

Re-measurement of Internal Friction Curve of Specimen (Cu-8.91 w/o Al) Annealed 50 Hours at 700°C (Torsional Pendulum One).

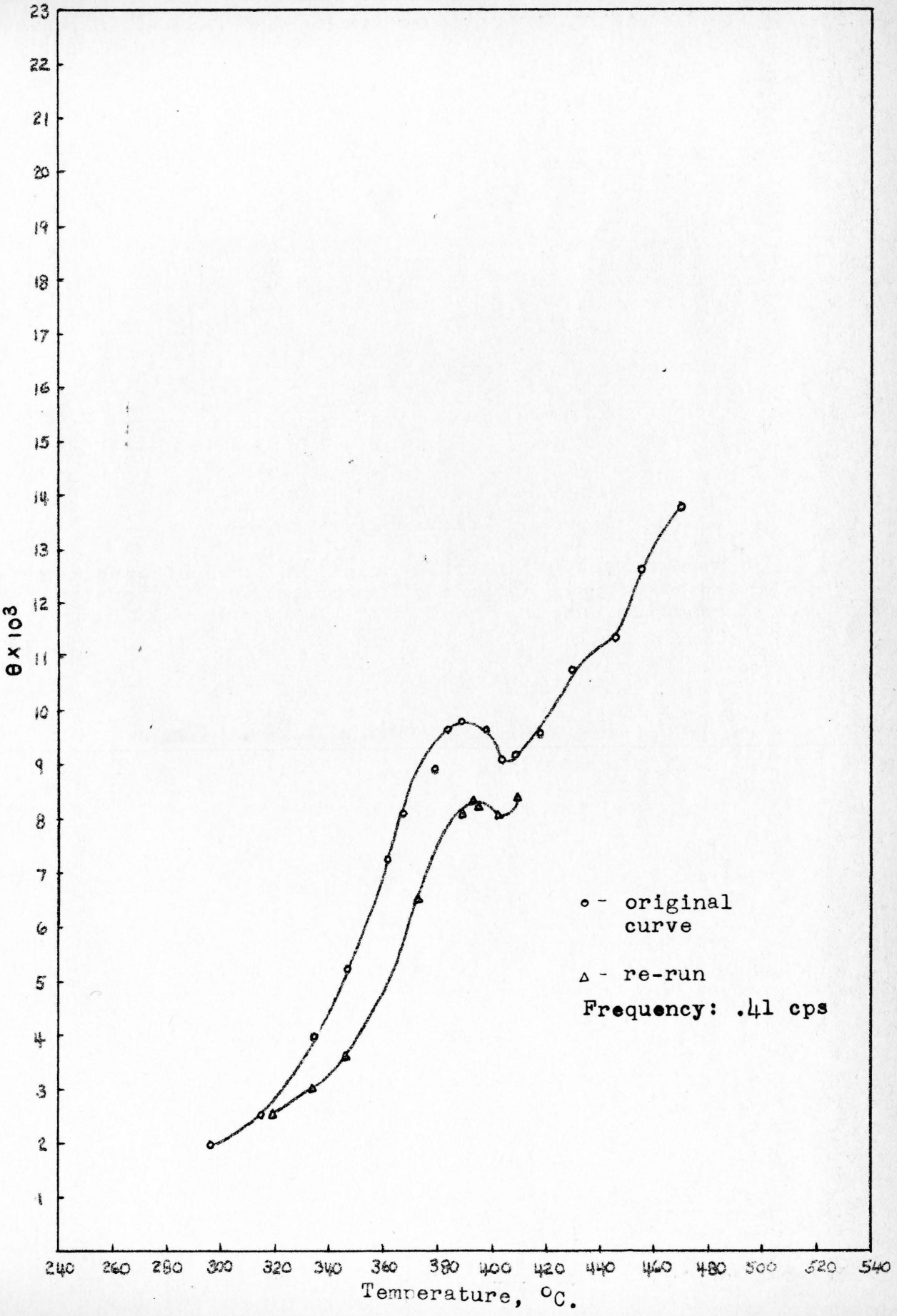
θ X 10³
23
22
21
20
19
18
17
16
15
14
13
12
11
10
9
8
7
6
5
4
3
2
1
240
260
280
300
320
340
360
380
400
420
440
460
480
500
520
540
Temperature, °C.
o - original curve
Δ - re-run
Frequency: .41 cps

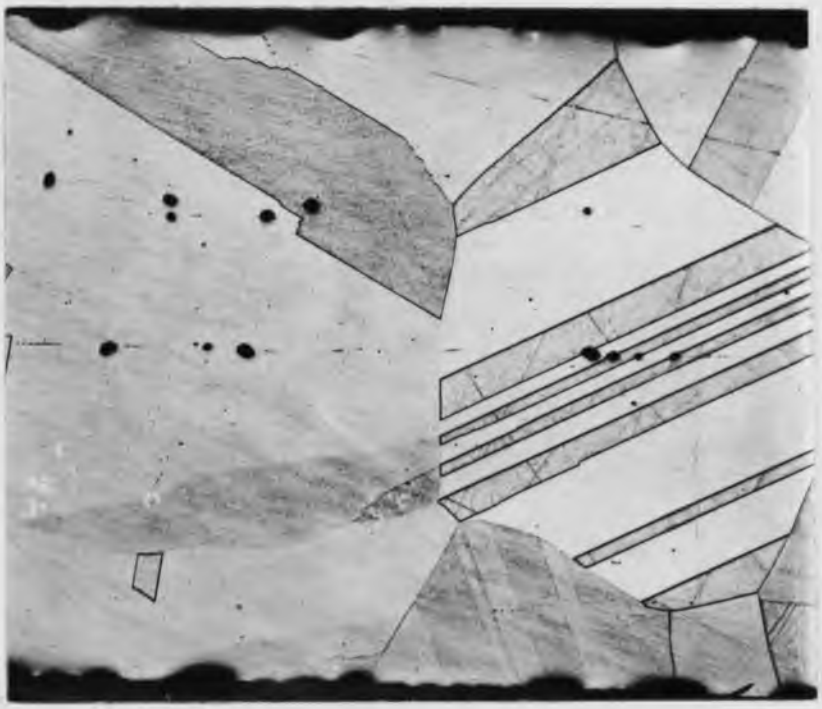

100X FeCl Etch

Figure 22

Grain Size of Specimen (Cu-8.91 w/o Al) Annealed 50 Hours at 700°C used in Section One.

Figure 23

Internal Friction Curve of a Specimen (Cu-4.91 w/o Al) Annealed 24 Hours at 950°C (Torsional Pendulum Two).

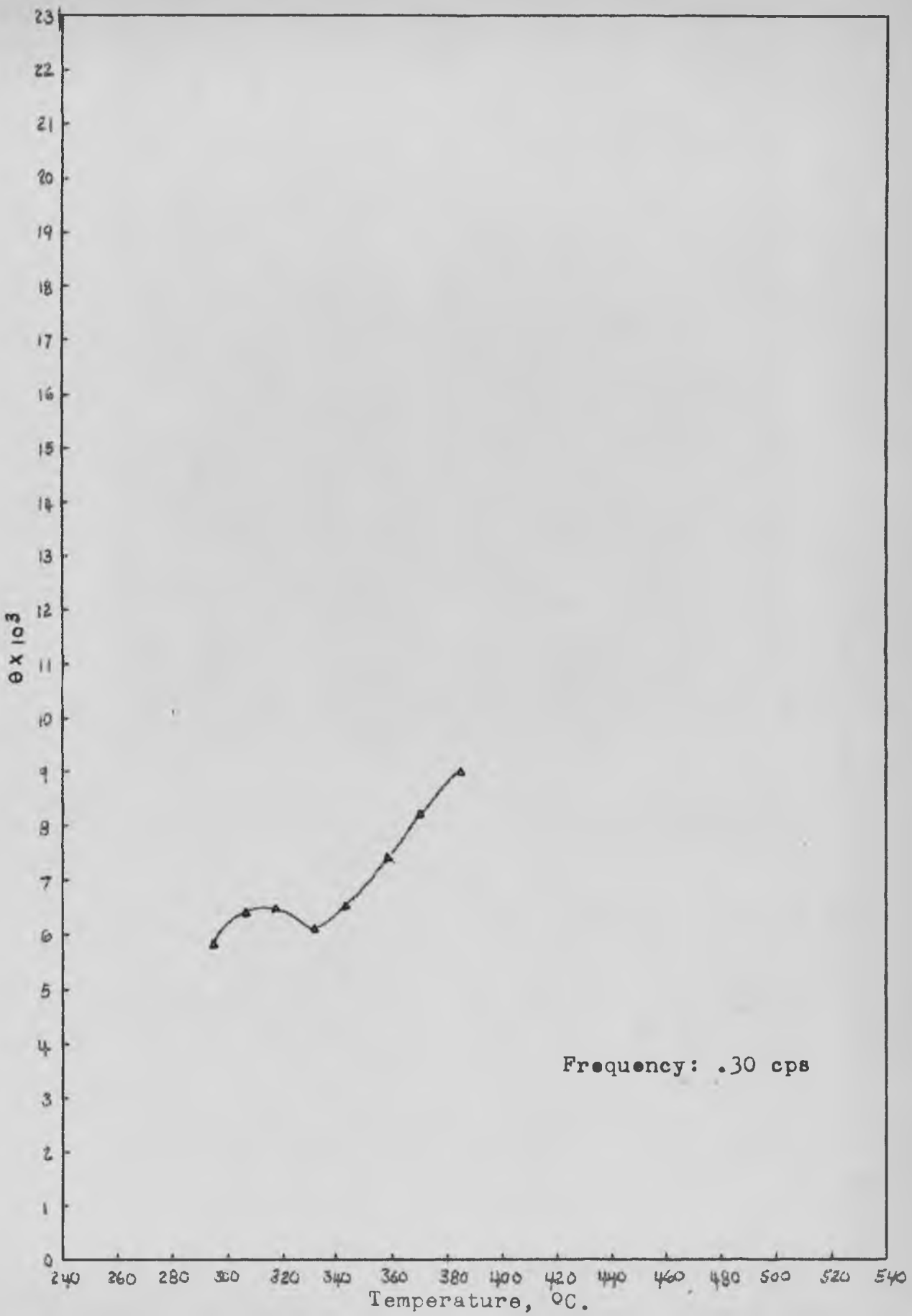
θ X 10³
0
1
2
3
4
5
6
7
8
9
10
11
12
13
14
15
16
17
18
19
20
21
22
23
240
260
280
300
320
340
360
380
400
420
440
460
480
500
520
540
Temperature, °C.
Frequency: .30 cps

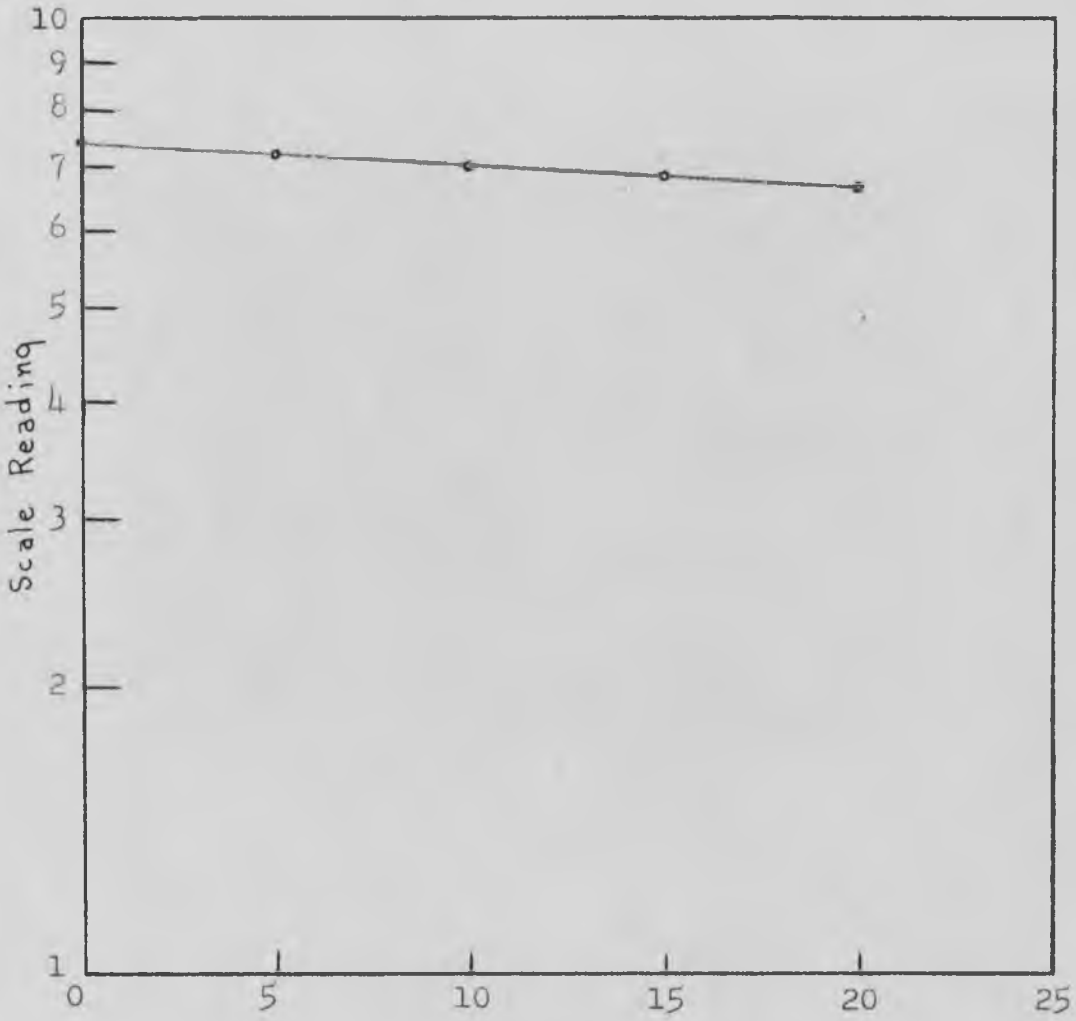

Figure 24

Sample Plot of a Set of Scale Readings
on Semi-Log Paper.

Figure 25

Elastic After-Effect Curve of a Cu-15 a/o Zn Specimen (Annealed 48 Hours at 750°C) Measured at 260°C.

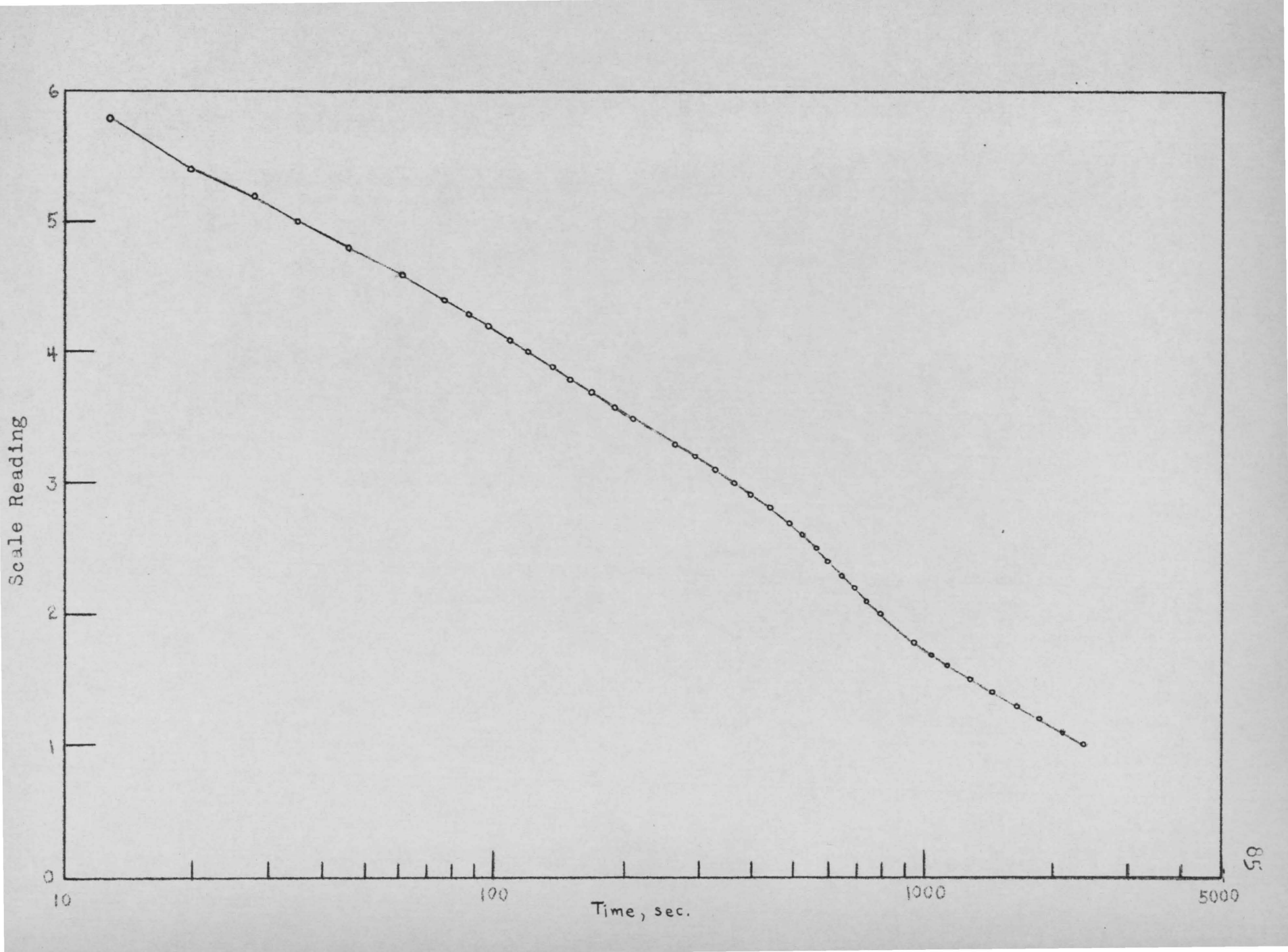
Scale Reading
0
1
2
3
4
5
6
10
100
1000
5000
Time, sec.